NATURAL ANTIBIOTIC PRODUCTION

MQP Final Report

WPI

Natural Antibiotic Production

A Major Qualifying Project Report:

Submitted to the Faculty of

WORCESTER POLYTECHNIC INSTITUTE

in partial fulfillment of the requirements for the

Degree of Bachelor of Science in:

Biochemistry

Lauren Herchenroder
Alexander Pratt
Jordyn Van Minos

Project Advisors:
Professor Mike Buckholt, BBT
Professor Christopher Lambert, CBC

5/6/2021

Table of Contents

Acknowledgements

We would like to express our sincere gratitude to the Chemistry and Biochemistry department, as well as the Biology and Biotechnology department for funding our project. Special thanks to our advisors Professors Michael Buckholt and Christopher Lambert, who guided us through the project.

Section 1: Abstract

As bacteria continue to evolve, several species have adopted increasingly advanced antibiotic-resistant qualities. These multi-drug resistant (MDR) bacteria pose a threat to the medical field where the invention of new antibiotics is constantly underway in efforts to plateau the effects of potentially dangerous bacteria.

Our Major Qualifying Project focuses on the production of antibiotics from isolated bacteria retrieved from select microenvironments found in soil. This research was conducted using samples collected from our group in 2019 and continued through the duration of our senior year. We determined the effects of our isolate's antibiotic production capabilities using ESKAPE safe relatives and other safe relatives, noting inhibition against *Mycobacterium smegmatis*. We then attempted to identify the genus of our isolate using PCR to amplify the 16S rRNA gene. To confirm the genus of our isolate, we moved forward to a full genomic extraction.

Subsequently, we attempted to isolate the proposed antibiotic-producing agent through organic extraction, followed by HPLC. We found clear separations through our organic solvents, and our HPLC runs produced multiple fractions that were used to test the success of our isolation. Ultimately, no clear signs of inhibition were recorded by these means, and we were unsuccessful in confirming the antibiotic capabilities of our isolate.

Section 2: Introduction and Background

2.1 Rise in Multi Drug Resistant Bacteria

The first antibiotic that was developed from bacteria was Gramicidin A, which destroys the bacterial cell membrane, and was isolated from *Bacillus Brevis,* commonly found in soil (Mendelsohn 2002). The rate at which new antibiotics have been discovered has rapidly declined. This marks an alarming trend as multidrug resistant (MDR) bacteria become a more common threat to medicinal practices. Every year, MDR bacteria have resulted in a total of 700,000 deaths worldwide (Adrizain, 2013). The decline in antibiotic discovery is directly tied to this growing threat of MDR strains. The new pharmaceuticals simply cannot keep up with nor compete with these highly resistant species of bacteria. External factors, including a lack of funding for projects to synthesize drugs, also contribute to a lack of new antibiotics. Conducting research to discover new antibiotics, despite this lack of funding, remains an important aspect towards combating the increasing prevalence of MDR bacteria (Adrizain, 2013).

2.2 Bacterial Composition and Cellular Components

Compared to eukaryotes, bacteria are simplistic organisms that hold a wide range of specific functions and roles. Bacteria are single-celled, meaning cell shape is critical in the determination of their function (Voet et. al, 2016, 7). Eukaryotes have a more complex cell composition with smaller organelles encased in cellular membranes. Bacteria lack these membrane-bound organelles, and instead keep their contents protected within a plasma membrane and an additional cell membrane. The plasma membrane offers protection to the cell and acts as a selective barrier for trafficking substances through the organism. As described by the fluid-mosaic model and based on hydropathy of the membrane, the phospholipid bilayer along with embedded/attached proteins can mediate transport. They function in concert as a semipermeable barrier to traffic materials and maintain cell function (Voet et.al., 2016, 269).

Located just outside of the plasma membrane lies the cell wall. Like the plasma membrane, the cell wall also provides protection to the cell and maintains cellular traffic. The cell wall provides strength and rigidity to maintain the bacteria's shape and helps determine its growth, reproduction, and nutrient abstraction patterns (Voet et. al, 2016, 7).

Two main categories used to distinguish bacteria are gram positive and gram negative. Differences in the peptidoglycan composition of the cell wall yield different properties that tie into metabolic processes. Peptidoglycan is composed of two glucose derivatives and depending on the properties of the bacteria the peptidoglycan can form various layer structures (Voet et. al, 2016, 339). Polysaccharide peptidoglycans compose a large portion of the bacterial cell wall.

Gram positive bacteria have many layers of peptidoglycan along with the glycopolymer, teichoic acid (Romaniuk & Cegelski, 2015, 1). Teichoic acid acts as a lipid anchor that supports the integrity of the cell and causes a negative net charge on the cell wall to aid in the synthesis of ATP, which provides energy to aid in reproductive rates (Bruslind, 2021, 28).

Gram negative bacteria have an even more complex composition despite having less layers of peptidoglycan. The bulk of the cell wall includes the plasma membrane, positioned directly outside the peptidoglycan layers (Hernandez et al.,71). Similar to the function of the cell wall in gram positive bacteria, these layers also provide the cell wall with rigidity and greater reproductive rates. The outer membrane is composed of a lipid bilayer resembling those of a typical cell membrane, with the exception being the presence of lipopolysaccharides (LPS) in the outer membrane.

Lipopolysaccharides yield a negative charge for the cell that helps to stabilize the outer membrane by blocking access of harmful chemicals into the cell wall (Bruslind, 2021, 29). This charge is also seen in gram positive bacteria for similar reasons to some degree. LPS plays a role in both immunity and the production of antibiotics in a cell. Additionally, LPS contributes to cellular trafficking. In order to pass the LPS, periplasmic enzymes must first break down the larger substances that cannot pass this layer (Raetz & Whitfield, 2002). From there, the broken-down molecules may pass through porins, and other transmembrane proteins found in the peptidoglycan layers. Given this ability to traffic chemical materials, LPS is able to trigger “an immune response in an infected host, causing the generation of antibiotics specific to that part of the LPS" (Bruslind, 2021, 29). This trafficking through the outer membrane is correlated to antibiotic resistance. Such permeability impacts the susceptibility to antibiotics that target intracellular processes. For example, “small hydrophilic drugs, such as beta-lactams, use the pore-forming porins to gain access to the cell interior” (Delcour, 2009, 808). After entering the cell’s interior, these drugs facilitate chemical reactions that effectively destroy the cell from the inside out, inhibiting its growth and reproduction.

In response to the hydrophilic drugs, bacteria have developed a range of drug-resistant properties to pump the drugs back through the efflux pumps out of the cell membranes (Delcour, 2009, 808). LPS also aids in resisting outside antibiotics and other foreign molecules that could harm the bacteria. LPS does this using similar trafficking methods employed to expel the antibiotics produced within the bacteria. This provides, “a barrier to hydrophobic antibiotics and other compounds, and the [bacterial] strains which express full length LPS have an intrinsic resistance to these [antibiotics]" (Delcour, 809).

2.3 Bacterial Growth Patterns

Reproduction is particularly important in the research field for bacteria; faster reproduction rates allot for more genetic experimentation with shorter wait times in between each growth cycle. Bacteria owe their quick reproduction to their small size. The small surface-to-volume ratio specifically allows for their heightened reproductive speed (Voet et. al, 2016, 8). Therefore, bacteria are able to evolve faster and adapt to a wider range of modifications for survival (Bruslind, 2021, 23).

It is important to consider the growth conditions and patterns of different microbes during an experimental study, so that the microbe of interest thrives. Media types that are used to culture microbes in the lab are "enriched with a variety of organic molecules, macromolecules, and vitamins to support the growth of fastidious bacteria" (Hernandaz et.al, 2018, 43). Other parameters that are also important for the growth of microbes include oxygen levels, light exposure, pH, and temperature. The growth of these colonies follows a common path, illustrated using a growth curve (figure 1).

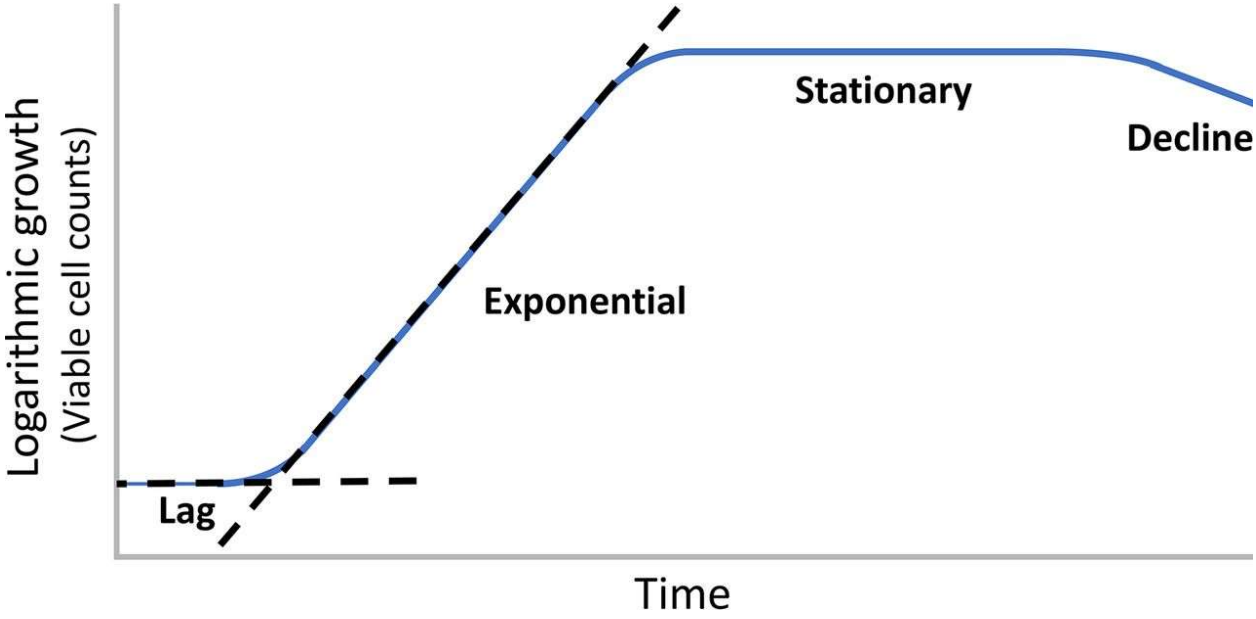

Figure 1: Growth Diagram for a bacteria life span (Bertrand, 2019).

Bacterial growth is estimated using the spectroscopic properties of suspended particles in a liquid culture over time. As the cell concentration increases, the solution will lose its clarity, and this 'cloudiness' can be measured by a spectrophotometer as optical density unit (ODs). When plotted, these ODs over time establish a standard growth curve, displaying the four main stages of the bacteria's life cycle (Hernandez et al., 2018, 50-51).

Each phase shown on the growth curve represents a point in the bacteria's life span. As time passes, the number of viable cells fluctuates and is correlated to the changes in ODs. The

exponential curve on the graph is known as the log phase and is representative of the cells reproducing exponentially with amble nutrients and space to grow. Preceding this curve is an initial plateau, known as the lag phase, and represents the initial transfer of the bacteria to a new medium. Another plateau is seen when the exponential log phase tapers off into the stationary phase. It is in this phase where nutrients of the media have started to deplete and room for more growth is limited, causing a stunt in cell growth. Finally, the cycle concludes with a drop off in the late stage of the plot. This stage signifies the death phase, also known as the decline phase, where bacteria begin to die off from a lack of available nutrients and overcrowding (Hernandez et al., 2018, 51)

Overcrowding leads to a depletion in available nutrients and is an issue when trying to identify potential antibiotic producing bacteria. As the bacterial growth begins to cover the media, neighboring colonies begin to crowd around each other. Overcrowding often leads to competition for resources among different bacteria, which may create areas of no growth in the media where nutrients have been depleted. However, there are also instances when no growth is observed around a singular colony, where its neighboring colonies do not approach it. These neighbors form a distinct ring of empty space around the single colony. Typically, this is an indication that the singled-out colony is producing an antibiotic that is inhibiting the growth of the surrounding isolates. It is possible that this inhibition is caused by over competition in a specific area that has leached out all the possible nutrients, as previously mentioned, however the presence of an antibiotic being produced by the lone colony is still a possibility for this behavior.

2.4 Signs and Production of Antibiotics from Bacteria

When a bacterium produces an antibiotic, either as a defense against its enclosing bacterial neighbors or to secure its stake in the limited available nutrients of the media, it prevents the growth of the surrounding bacteria. A common method of attack is to target or break down the opposing bacteria’s cell wall. Other methods of attack can include targeting specific functional proteins, or various processes that are essential to the bacteria's survival. This combination of offensive and defensive strategies is seen in the formation of zones of inhibition (ZOIs) (Hernandez et al., 2018, 64). Zones of inhibition can be caused by the bacterial production of antibiotics that populate onto the media which stunts the growth of approaching bacteria by targeting their cell walls. Below in figure 2, a LB plate is displayed with isolates that have formed what appears to be zones of inhibition against surrounding bacteria. These plates were cultured in 2019, and are discussed more in depth in appendix A.

Figure 2: Diluted (10^-2) LB plate. Experienced ample microbial growth, the red dots are colonies that exhibit possible zones of inhibition. These zones either displayed colonies growing in a curve-like fashion around a specific colony, or a colony that is surrounded by other colonies but does not come into direct contact with the surrounding colonies.

Similarly, in figure 3, are two examples of isolates that were able to form zones of inhibition against an ESKAPE safe relative, *P. putida.* ESKAPE is an acronym derived from the names of common pathogens, and these 'safe relatives' are their laboratory-safe versions. The ESKAPE pathogens include: *E. faecium, S. aureus, K. pneumoniae, A. baumannii, P. aeruginosa,* and Enterobacter species. These isolates (marked in red) were later characterized in a variety of chemical assays, and one of which was subsequently used in this project for a deeper analysis. The experimentation and results that led to these figures is discussed more in depth in appendices B and C.

Figure 3: PDA plate spread with the safe relative, P. putida*. Various isolates were patched onto the plate and two ZOIs (marked in red) have formed, indicating possible antibiotic production to inhibit the surrounding* P. putida *growth.*

Determining whether a lack of growth in a specific area is caused by overcrowding or by the production of an antibiotic requires additional testing. A common and reproducible test involves replating the colony of interest against known pathogens and observing whether similar behaviors are replicated or not. Antibiotics are one of many secondary metabolites that can be produced by bacterial gene clusters. These gene clusters have been found to produce antifungal agents, antitumor agents, immunosuppressants and cholesterol lowering agents, in addition to antibiotics (Fischbach, et al., 2008). It is important to consider that secondary metabolites are only a byproduct of secondary metabolic pathways. These metabolites are not the ones responsible for the regulation or functionality of the organism producing them. Instead, these metabolites contribute to the ecology and physiology of the organism (Fischbach, et al., 2008). One well known purpose of secondary metabolites is their role as forms of communication between microbes, and between microbes and multicellular organisms. This suggests that these metabolites have been responsible for a large portion of their producers' evolutionary pathway. To prevent overextending their resources and energy reserves, some bacteria will produce a secondary metabolite as a signaling molecule to assess the surrounding populations and report back to the bacteria (Romero, et al., 2011). These types of metabolites allow the bacteria to have advanced knowledge of its surroundings in order to produce specific metabolites in the right quantity, and gain an advantage in their environment (e.g., producing antibiotics to stunt growth of surrounding bacteria to better compete for resources).

2.5 Antibiotic Resistance

Being able to synthetically reproduce or improve upon various secondary metabolites, without needing the bacteria to produce them, is a key step for the future of antibiotic production. Understanding the intricacies of secondary metabolite production will allow us to tackle the rise in multidrug resistant (MDR) strains, pan-drug resistant (PDR) strains, and compensate for the drop in new antibiotics being discovered.

Most of the antibiotics we use today come from actinomycetes strains of bacteria found in soil. However, it is estimated that not even 1% of the total amount of bacteria in soil have been studied. Most frequently, only the bacteria producing metabolites that inhibit other bacteria or fungi are chosen, thus leaving countless other strains unresearched (Clardy & Walsh, 2004). Considering this, endophytes have recently been used to develop over 30 different antibiotics to help broaden this research field (Strobel & Daisy, 2003).

The reason the exploration for naturally produced antibiotics has slowed over the years is largely due to two reasons. First, not every bacterial infection calls for the use of antibiotics as some are often taken care of through our immune systems (Grant & Hung, 2013). This plays into the second reason, where the low overall usage of antibiotics compared to other 'over the counter' drugs results in low overall revenue (Fischbach & Walsh, 2009). Many companies have turned their efforts towards modifying existing antibiotics versus searching for new ones. However, the rise in multidrug and pan-drug resistant strains continues to climb as they compete against "synthetically tailored successive generations of antibiotics" that have been around for ages (Fischbach & Walsh, 2009).

Antibiotic resistant bacteria go through different stages in order to develop from their more vulnerable counterparts. The first of these steps is the emergence of resistance factors. Mutations in the bacterial gene code may occasionally produce structural or chemical means to resist the antibiotic's lethal potential (Fischbach, et al., 2008). Developing resistance to an antibiotic, allows an individual bacterium to increase its chance of survival in an environment saturated with the antibacterial compound. These resistance factors allow the bacteria with the mutated gene to mobilize, propagating throughout the area surrounding it until the resistance factor occupies larger parts of the population. These bacteria evolved from host to host until these resistance factors became a dominant strain within succeeding generations. A possible step for the development of antibiotics includes a horizontal transfer of these resistance factors (Bengtsson-Palme, et.al., 2017). Horizontal gene transfer relays the same resistance capabilities to other pathogenic bacteria in the same area. The pathogenic strain disseminates through bacterial pathways. As the new resistant pathogen propagates, any other system that develops a different pathway towards resistance helps to make the bacteria's defense even stronger (Bengtsson-Palme, et.al., 2017).

2.6 Purification of an Antibiotic from Bacteria

To assess the potential of an isolate producing an antibiotic, ESKAPE safe relatives are grown in the presence of the isolate in question. ESKAPE safe relatives are bacterial strains similar to other known pathogens but are safe to use in a research laboratory setting. In the table 1, below, a chart is supplied that corresponds each safe relative to their known pathogen; the chart includes some non-ESKAPE bacterial strains that are also safer versions of different known pathogens (for example, *mycobacterium smegmatis).*

Table 1: ESKAPE Pathogens Chart

MDR Bacterial Strain	*Enterococcus faecium*	*Staphylococcus Aureus*	*Klebsiella Pneumoniae*	*Acinetobacter Baumannii*	*Pseudomonas Aeruginosa*	*Enterobacter Species*	*Mycobacterium Tuberculosis*
Safe Relative	*Bacillus Subtilis*	*Staphylococcus Epidermidis*	*Escherichia Coli*	*Acinetobacter Baylyi*	*Pseudomonas Putida*	*Enterobacter Aerogenes*	*Mycobacterium Smegmatis*
Reference Number	2	3	4	5	6	7	9

Chart of ESKAPE safe relatives and other safe strains of known bacterial pathogens.

If growth of the ESKAPE safe relative is stunted with the formation of a zone of inhibition around the isolate in question, then there is a possibility that an antibiotic produced from the isolate of interest is the main cause of inhibition. This isolate can then be subjected to further testing for confirmation of its antibiotic-producing capabilities.

Identifying the genus of an unknown isolate, helps to characterize an unknown sample based on similar strains of known bacteria. Through PCR, the DNA sequence of the 16S rRNA gene in a sample can be amplified after implementing different thermocycling procedures to help denature the bacteria and help express this gene of interest. The 16S rRNA gene sequence is a common genetic marker in bacteria because it is expressed in nearly every bacterium, typically as a multigene family. The 16S rRNA gene's function is also conserved, so random mutations in this sequence provide an accurate estimate of evolution for the species of interest (Janda & Abbott, 2007). After amplification by PCR, the sample may be run through an agarose gel during electrophoresis where the charged field supplied by two electrodes separates the sample based on the DNA's negative charge and the size of the sample. After the run, the sample sequence for the 16S rRNA gene should span around 1500 base pairs, which is long enough to study its bacterial informatics (Janda & Abbott, 2007). After obtaining the DNA bands around this mark, they may be sent off for sequencing. The sequence can then be sent through BLAST, a bioinformatics program that compares biological sequence information, in order to identify the genus of the unknown isolate.

After its identification, the isolate may then be subjected to two forms of extraction to attempt to isolate the antibiotic from the isolate. The use of organic solvents, namely methanol and ethyl acetate, may be used as a first step towards this isolation. The organic solvents help to degrade the bacterial cell wall and release the metabolic components associated with antibiotic-production into the liquid solvent. This liquid layer contains the antibiotic that can be tested against different strains of known bacteria to assess its inhibition ability and strength. Further purification of this antibiotic can be processed through the use of high-pressure liquid chromatography (HPLC).

HPLC is a form of column chromatography where the sample is pushed through a stationary phase by a mobile phase using increased pressure. Extracts from organic solvents may be transferred to a HPLC column to further separate out the antibiotic-producing metabolite. HPLC can be used to isolate a specific extract and determine its purity. In figure 4, below, underneath the three panels, the program will report written responses of the purity analysis report. The first report is the decided purity factor. It will either state that the factor exceeds the calculated threshold limit or is within the calculated threshold limit. Other information given includes the number of spectra that exceed the threshold, the calculated purity factor and threshold, the reference of the peak, the number of spectra, and the noise threshold (Stahl, 2003). The program is also intelligent enough to adjust the readings before analysis to correct for background noise and absorption typically caused by the mobile phase. The primary signal labeled A by the program is in the deep UV range emitting around 246 nm, the second signal labeled B is also in the UV range emitting around 285 nm, and the last signal is in the low end of the visible light range emitting around 330 nm. In figure 4, the top panel is an overview of the run detected by the primary signal A, the bottom left panel is a recording and comparison of the spectra of the peak, and the bottom right panel displays the calculated peak purity ratio. Each peak seen in the overview of the run is analyzed, however only the collected peak is of importance to this report and can be identified by the red box outlining the peak.

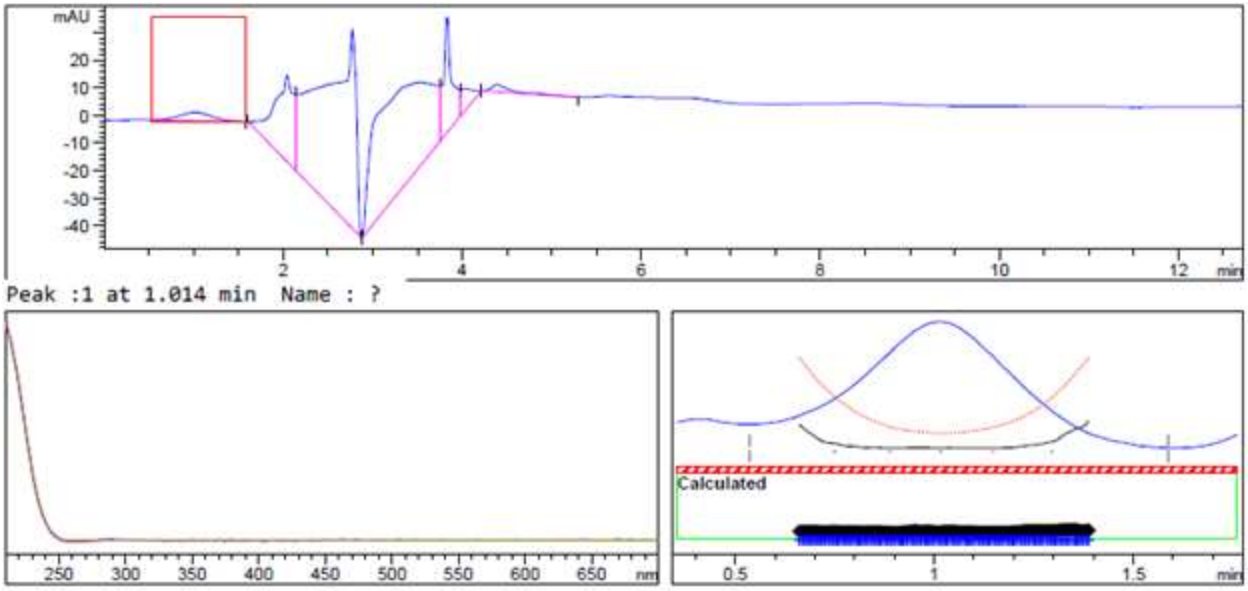


```
-> The purity factor is within the calculated threshold limit. <-

Purity factor : 999.852 (110 of 110 spectra are within the calculated threshold limit.)
Threshold     : 996.229  (Calculated with 110 of 110 spectra)
Reference     : Peak start and end spectra (integrated) (0.534 / 1.588)
Spectra       : 5  (Selection automatic, 5)
Noise Threshol: 0.123  (12 spectra, St.Dev 0.0576 + 3 * 0.0219)
```

Figure 4: Example purity analysis calculated automatically by the HPLC program.

The goal of the purity analysis is to identify the number of compounds in the peak through diode-array detection. When a peak is considered impure, the presence of multiple compounds in the sample have been detected. Typically, when multiple compounds are present in one peak they do not vary drastically in chemical structure, but the spectra will be shifted either left or right and can have various amplitudes. The greater the difference in spectra, the greater the difference in the compounds. Occasionally, there are small variations in a pure spectrum. For example, a difference in the amplitude of pure spectra usually indicates a difference in concentration. In figure 5 below, we can see examples of pure and impure spectra.

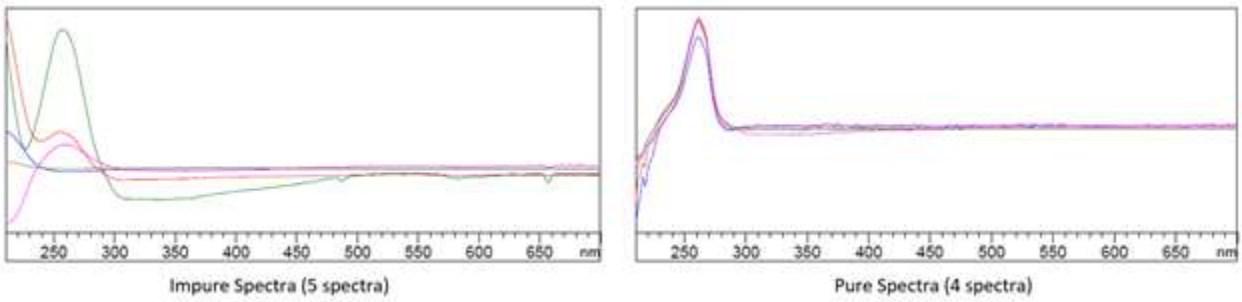

Figure 5: Pure and impure spectra examples. Readings in the pure example (right) are almost identical compared to the vast differences in spectra of the impure example (left). The program uses various colors to show the different spectra used in the calculations.

The bottom right panel of figure 6 is where we can see a visualization of the threshold and similarity curves in comparison to the analyzed peak. The similarity curve is calculated based on a comparison of all spectra to one or more spectra depending on the user's preference (Stahl, 2003). The program we used compares all spectra to the peak start spectra and the peak end spectra. The threshold curve is then calculated in order to understand the effect of background noise on the similarity (Stahl, 2003). The presence of background noise will not determine the purity analysis outcome, but the similarity curve can indicate the presence of impurities. As previously mentioned, this is important in situations where spectra are very similar or identical even when impurities are present. In figure 6 below, are examples of what pure and impure similarity curves and threshold curves may look like.

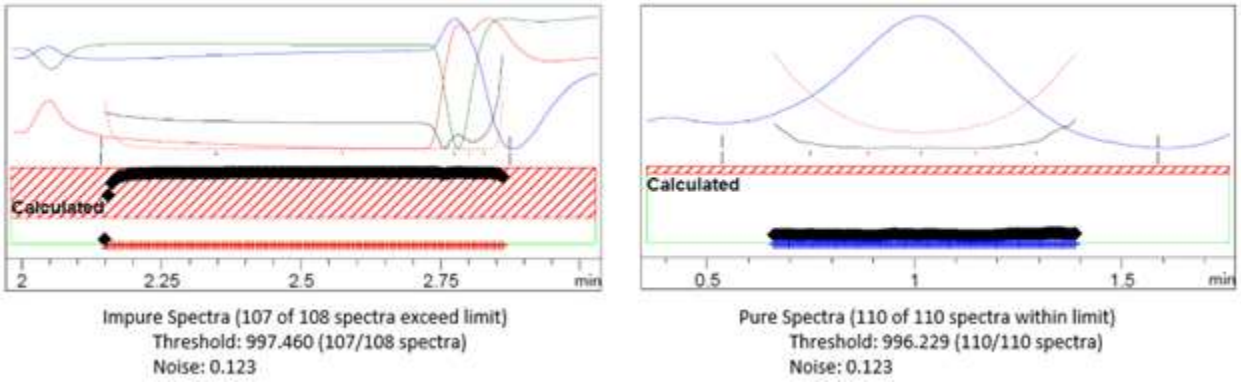

Figure 6: Pure and impure examples with calculated threshold and similarity curves. Factors used for calculations are listed below each image. To exceed or be within limit is in reference to the calculated threshold. Noise is consistent between examples, most likely because examples are from the same sample run.

2.7 Our Project

Our MQP aims to extract the antibiotic-producing element from our selected bacteria sample, 19-6 (labelled corresponding to the year it was collected, 2019, and our previous group number, 6). We will be employing the previously mentioned techniques to identify and extract a proposed antibiotic from 19-6, which was prepared by our group during a previous research project conducted in 2019 under Professor Buckholt's supervision. This isolate held many properties we believed would make for an interesting MQP and a smooth transition from a classroom setting to an independent research project. 19-6 was subjected to different chemical assays in the previous years. It was determined to be a gram-negative bacterium after multiple gram staining trials in addition to a MacConkey plate experiment. It is also oxidase negative, catalase negative, lactose negative, no fermentation of H_2S after a TSI tube experiment, lysine positive and indole negative, as determined by a MIL tube experiment, as well as amylase negative and starch positive following a starch plate experiment. These assays are discussed in detail in the appendix C as they were not conducted as a part of this MQP but did help in the characterization of our isolate.

Our MQP focused on confirming the antibiotic-producing capabilities of 19-6 after being frozen for one year. After this confirmation, our team moved to identifying the genus of 19-6 through the implementation of PCR and gel electrophoresis using the 16S rRNA gene. Afterwards, our group attempted to extract and purify the functioning antibiotic via organic solvents and HPLC.

We would like to mention that our MQP was completed with the limitations put in place by WPI during the Covid-19 pandemic. In these circumstances, our lab access was greatly restricted for long periods of time, and communication was often made difficult between supervisors and students with social distancing protocols in place. Keeping this in mind, our group had planned on a different route for our MQP, however, we had to adapt to the uncertainty of the semesters as they came. Nonetheless, our team had overcome many of these obstacles and were able to perform laboratory experiments for the full year, regardless.

Section 3: Methods and Procedures

As bacteria continue to evolve, several strands have adopted advanced antibiotic-resistant qualities. These multi-drug resistant (MDR) bacteria pose a threat to the medical field where the invention of new antibiotics is constantly underway in efforts to plateau the effects of potentially dangerous bacteria. A large focus of this research focuses on the production of antibiotics from isolated bacterial strains found in soil. Our bacterial strain, referred to as 19-6, was selected out of a group of 13 isolated bacterial strains. Multiple experiments were performed in order to determine the bacterial composition of 19-6, to concentrate the antibiotic produced by 19-6, and to test the purified antibiotic's chemical properties (refer to appendices A through C). The purified antibiotic will be tested against different safe relatives of well-known pathogens to understand more of its characteristics and potential.

Objectives

I. Test the effectiveness of 19-6 against other strains of bacteria
    a. Plate selected isolates from previous years on preferred media types to test viability of bacteria.
    b. Plate ESKAPE safe relatives and *M. smegmatis*.
    c. Plate 19-6 against previous years isolates, ESKAPE safe relatives, and *M. smegmatis* on both LB and PDA plates.
    d. Search for the appearance of zones of inhibition around 19-6.

II. Identify the 16S ribosomal gene of 19-6
    a. Perform PCR to replicate 16S rRNA encoding region of 19-6.
    b. Use gel electrophoresis to separate 16S rRNA bands from remaining primers and other DNA regions.
    c. Excise and purify band contents to send for sequencing and perform BLAST.
    d. Complete a full genomic DNA extraction to confirm genus.

III. Identify the antibiotic produced
    a. Perform organic extractions of the proposed antibiotic secreted by 19-6.
    b. Run high pressure liquid chromatography (HPLC) of 19-6 organic extracts.

IV. Assess the activity of the isolated antibiotic.
    a. Load isolated antibiotic from HPLC onto sterile disks.
    b. Use antibiotic disks to inhibit ESKAPE safe relatives and *M. smegmatis*.

Below is a flow chart of each objective pertaining to our research with brief results and conclusions.

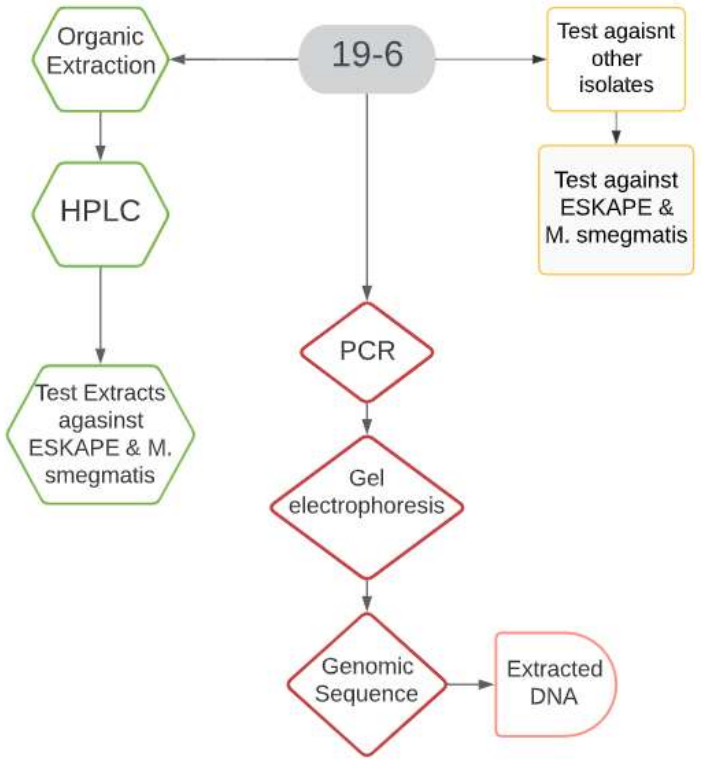

Figure 7: A flow chart of this project's experimentation and results.

(Unless otherwise stated, the following protocols were adapted from Tiny Earth - A research guide to studentsourcing antibiotic discovery *by Simon Hernandez, et.al.)*

3.1 Test the Effectiveness of 19-6 Against Other Strains of Bacteria

3.1.1 Plate selected isolates on preferred media types

Obtained past years isolates from the freezer to thaw and plate on their preferred media (refer to table 2 below). Labelled plates by their codes using the year the plates were cultured and by the number assigned to them by previous group projects (for instance: year-group number). Pipetted 100ul of each isolate onto their respective plates and spread using glass beads. The beads were immediately discarded after use. Grouped the plates by year and incubated at 37℃ for two days.

Table 2: Past Media Isolates Chart

Code	Name	PCR sequence	ZOI with colony	ZOI in Extraction	Putative genus and species	Best medium	Growth temp (°C)
2016-05	Amanda Moulaison	Yes	Yes	Yes	Pseudomonas Koreensis	TSA	-
2016-10	Mina Henes	Yes	Yes	Yes	Bacillus Subtilis	R2A	-
2016-16	Haylea Northcott	Yes	Yes	Yes	Bacillus	LB	-
2017-01	Brittany Jette	Yes	Yes	Yes	Bacillus	TSA	-
2017-02	Brittany Jette	Yes	Yes	Yes	Pseudomonas	TSA	-
2017-03	Emily Gordon	Yes	Yes	Yes	Paenibacillus	TSA	-
2017-03	Emily Gordon	Yes	Yes	Yes	Paenibacillus	TSA	-
2017-05	Johan Girgenrath	Yes	Yes	No	Paenibacillus	LB	-
2017-14	Lara Schmoyer	Yes	Yes	No	Paenibacillus	TSA	-
2018-14	Yvonne Niebuhr & Ilaria Wernick	Yes	Yes	Yes	Aneurinibacillus Aneurinilyticus	LB	37
2018-27	Erin Bryan	Yes	Yes	Yes	Delftia	LB	18
2018-77	Ryan Peters	Yes	Yes	Yes	Pseudomonas	R2A	37
2019-06	Jordyn Van Minos & Lauren Herchenroder	Yes	Yes	No	*Unknown*	PDA	26

The codes and descriptions of past years' isolates used to culture new plates of their colonies.

3.1.2 Plated 19-6 against past years isolates

Patch/Patch Protocol

After incubation to allow for full growth on a plate discussed in section 3.3.1, the patch/patch method was used to examine any possible formation of zones of inhibition caused by the isolate 19-6 against the other isolates from past years. An area on the outside of each of the plates was marked, using a permanent marker, to define where isolate 19-6 would be inoculated. Using a sterile inoculating loop, a colony from the 19-6 plate was transferred to the circled area on each plate of the select bacterial isolates from previous years. These plates were then put in

the incubator at 37℃ for two days to allow for growth and potential inhibition of past years' isolates to form.

Spread/Patch Protocol

100ul of liquid samples from each isolate of previous years were transferred onto their preferred media types and spread using glass beads. The glass beads were discarded after spreading. Next, using a sterile inoculating loop, a colony from isolate 19-6 was transferred onto these plates in a recognizable pattern. The spread/patch plates were incubated at 37℃ for two days to allow for growth and inhibition.

A second trial was conducted using PDA media (the preferred media for 19-6) for each of the previous years' isolates.

3.1.3 Plated 19-6 against ESKAPE safe relatives and *M. Smegmatis*

LB plates

100ul of ESKAPE safe relatives (*B. subtilis, S. epidermidis, E. coli, A. baylyi, P. putida, E. aerogenes)* and *M. smegmatis* were transferred onto LB plates. The liquid was spread evenly across the plates using glass beads, which were removed after spreading and later discarded. Then, 19-6 isolate was transferred onto each plate, using a sterile inoculating loop, in a recognizable pattern. The plates were incubated for two days at 37℃ to allow for growth and inhibition. This procedure was carried out in duplicate.

PDA plates

100ul of ESKAPE safe relatives (*B. subtilis, S. epidermidis, E. coli, A. baylyi, P. putida, E. aerogenes)* and *M. smegmatis* were transferred onto PDA plates. The liquid was spread evenly across the plates using glass beads, which were removed after spreading and later discarded. Then, 19-6 isolate was transferred onto each plate, using a sterile inoculating loop, in a recognizable pattern. The plates were incubated for two days at 37℃ to allow for growth and inhibition. This procedure was carried out in duplicate.

Controls

Seven PDA plates and seven LB plates were labelled accordingly to grow ESKAPE safe relatives (*B. subtilis, S. epidermidis, E. coli, A. baylyi, P. putida, E. aerogenes*) and *M. smegmatis*. 100ul of each safe relative was transferred to their appropriate plate and left to incubate at 37℃ for two days.

3.2 Identify the 16S Ribosomal Gene of 19-6

3.2.1 PCR and gel electrophoresis

Method 1:

Transferred 19-6 colony to 100ul of sterile water using sterile toothpicks. Boiled solution for 10 minutes, afterwards placed boiled solution into an ice bath for 10 minutes; and repeated an additional cycle of this boiling/freezing interval. Transferred 11ul of boiled solution to a centrifuge tube, added 15ul of 2X one taq master mix and 4ul of the 16S primer mix (containing

1492R and 27FSSU, at 5uM). Sequence of primer 27F 5'-AGAGTTTGATCCTGGCTCAG-3'; sequence of primer 1492R 5'-ACGGCTACCTTGTTACGACTT-3' (Integrated DNA Technologies, 2021).

The solution was run in a thermocycler with the following conditions titled LAJ Program:

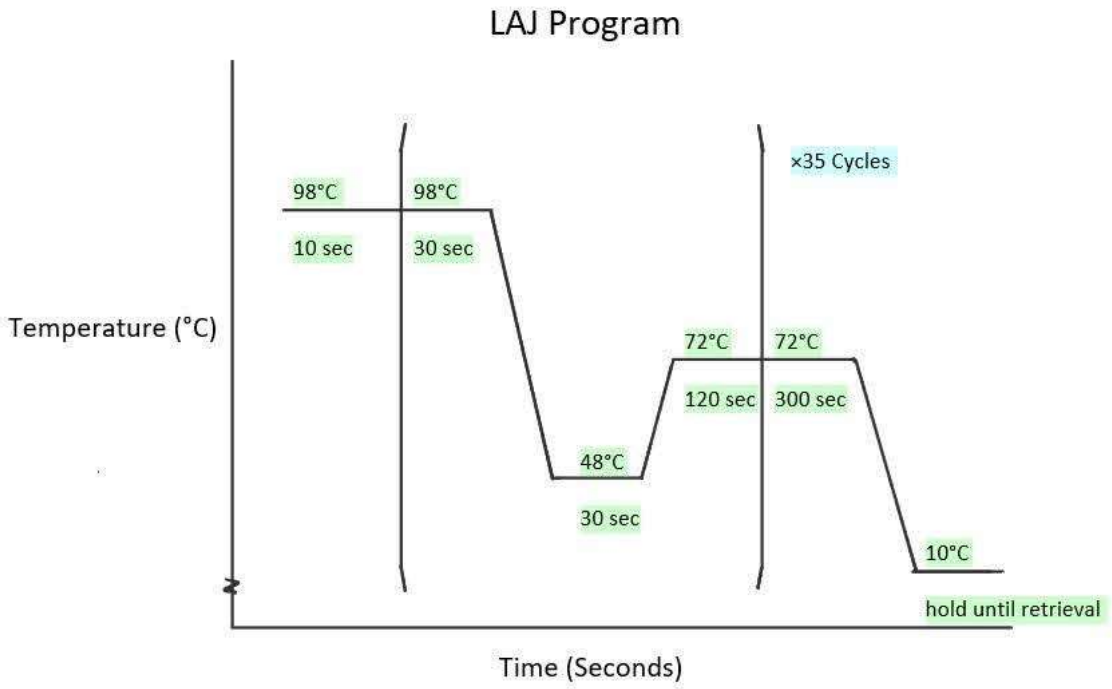

Figure 8: Thermocycling conditions for Method 1, titled LAJ Program, with a repeated annealing temperature of 48℃ for 35 cycles.

Prepped 1% agarose gel (1g agarose with 100ml of 1x TAE) for electrophoresis. The electrophoresis box was set at 120 volts for a 30-minute timer (Addgene, 2018). Loaded 5ul of hyper ladder in the leftmost well, and 10ul of the PCR products into wells from left to right. They were labeled 1 through 5, respectively. After 30 minutes of run time, a lightbox was used to visualize results with an ultraviolet wavelength. This method was completed in duplicate.

Method 2:

Transferred 19-6 colony to 100ul of sterile water. Boiled solution for 10 minutes, afterwards placed boiled solution into an ice bath for 10 minutes; repeated an additional cycle of this boiling/freezing interval. Transferred 11 ul of boiled solution to the centrifuge tube, added 4ul of the 16S primer mix (containing 1492R and 27FSSU, with 5uM concentration).

Ran solution in thermocycler with the LAJ Program conditions.

Prepped gel with 1% agarose gel (1g agarose with 100ml of 1x TAE), and added in 1ul dye to the gel itself in order to fluoresce the DNA bands of the PCR products. The electrophoresis box was set at 120 volts for a 30-minute timer (Addgene, 2019).

Loaded 5ul of hyper ladder in the leftmost well, and loaded 10ul of the PCR products into the wells from left to right. They were labeled 1 through 3 respectively. Observed bands under a light box and a ChemiDoc program.

Method 3:

Transferred 19-6 colony into 30ul of sterile water and boiled solution for 10 minutes, afterwards placed the solution into an ice bath for 10 minutes; repeated an additional cycle of this boiling/freezing interval. Transferred 11ul of the boiled solution to centrifuge tube, labelled A, and about 11ul of boiled solution to tube B. Both tubes (A and B) had 4ul of the 16S primer mix (containing 1492R and 27FSSU, at 5uM) added to their solution. Ran solution in thermocycler with the LAJ Program conditions.

(Note: PCR products A and B were run on the same gel for electrophoresis as PCR products C and D from Method 4 of PCR and gel electrophoresis)

Prepped gel with 1% agarose gel (1g agarose with 100ml of 1x TAE), and added in 1ul dye to the gel itself in order to fluoresce the DNA bands of the PCR products. Loaded 5ul of hyper ladder to the leftmost well and added 10ul of each PCR product from left to right. They were labeled A through D, respectfully. Ran gel at 110 volts for 1 hour. Examined bands under UV light box and Chemidoc program.

Method 4:

Transferred the 19-6 colony into 30ul of sterile water and boiled solution for 10 minutes, afterwards, placed the solution into an ice bath for 10 minutes; repeated an additional cycle of this boiling/freezing interval. Transferred 11ul of the boiled solution to centrifuge tube, labelled C, and 11ul of boiled solution to centrifuge tube, labelled D. 4ul of 16S primer mix (containing 1492R and 27FSSU, at 5uM) was added to tube C and about 4ul of 16S primer mix (containing 1492R and 27FSSU, at 5uM) was added to tube D.

The solution was run in a thermocycler with the following conditions titled LAJ 2 Program:

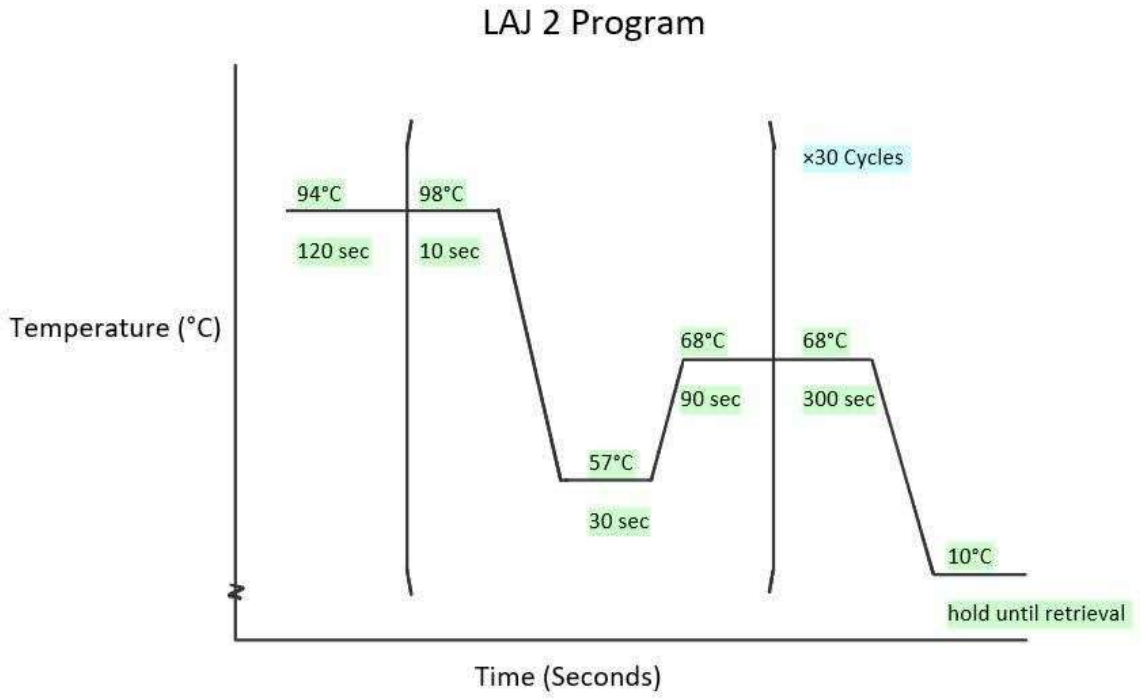

Figure 9: Thermocycling conditions for Method 4, titled LAJ 2 Program, with a repeated annealing temperature of 57℃ for 30 cycles.

(Note: PCR products C and D were run on the same gel for electrophoresis as PCR products A and B from Method 3 of PCR and gel electrophoresis)

Prepped gel with 1% agarose gel (1g agarose with 100ml of 1x TAE), and added in 1ul dye to the gel itself in order to fluoresce the DNA bands of the PCR products. Loaded 5ul hyper ladder to the leftmost well and added 10ul of each PCR product from left to right (A through D, respectfully). Ran gel at 110 volts for 1 hour. Examined bands under UV light box and Chemidoc program.

Method 5:

Transferred 19-6 colony to 30ul sterile water and boiled solution for 10 minutes. After boiling, placed the solution in an ice bath for 10 minutes; repeated an additional cycle of this boiling/freezing interval. Transferred 11ul of boiled solution into centrifuge tube, numbered 1, and transferred 11ul of boiled solution into centrifuge tube, numbered 2. Added 1ul of forward primer and 1ul of reverse primer for 16S rRNA into tube 1. Added 2ul of forward primer and 2ul of reverse primer for 16S rRNA into tube 2.

The solution was run in a thermocycler with the following conditions titled LAJ 3 Program:

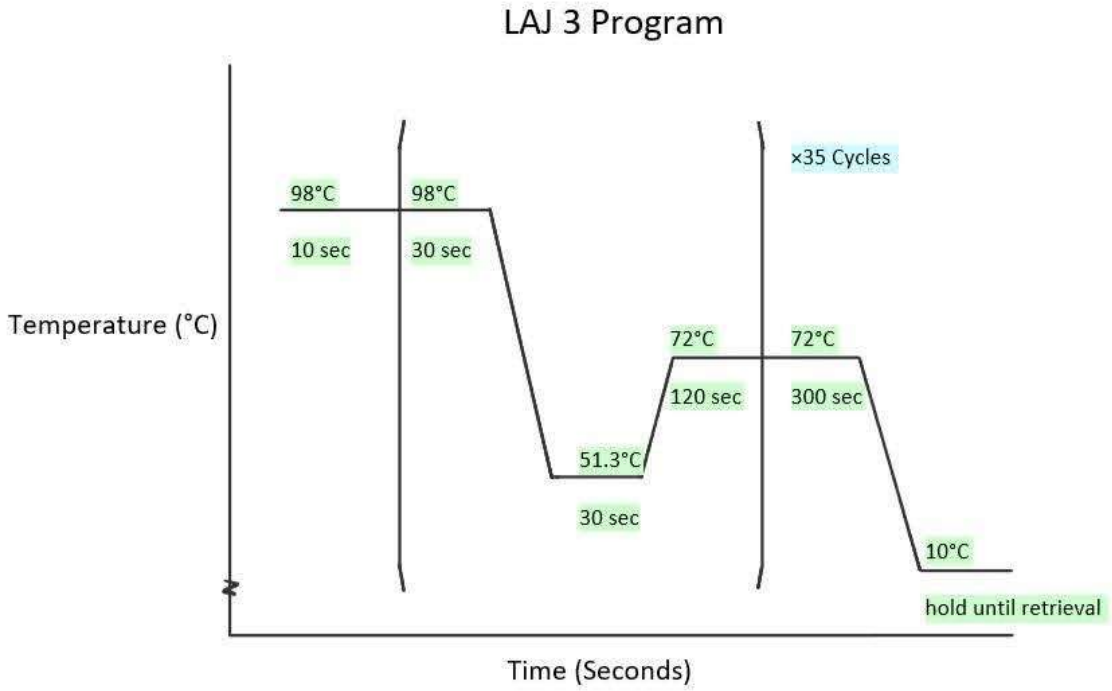

Figure 10: Thermocycling conditions for Method 5, titled LAJ 3 Program, with a repeated annealing temperature of 51.3℃ for 35 cycles.

(Note: The forward primer had a T_M of 55.2C and the reverse primer had a T_M of 57.4C. Here, "5C less than the T_M of primers" was used as stated by the primer source, Integrated DNA Technologies website, and the average of those two values was used for the forward and reverse primers to use in the thermocycling conditions.)

Prepped gel with 1% agarose gel (1g agarose with 100ml of 1x TAE), and added in 1ul dye to the gel before pouring to fluoresce the DNA in the PCR products. Loaded 10ul PCR products 1 and 2 (left to right, respectfully); loaded 5ul of hyper ladder in the leftmost well. Gel was run at 110 volts for 1 hour. Gel bands were examined under UV light and Chemidoc. This method was done in duplicate using an identical procedure as performed for tube 2 with the 2ul of forward primer and 2ul of reverse primer for 16S rRNA added.

Additionally, ran another trial using method 5 with the addition of 4ul of the 16S primer mix, instead of the separate forward and reverse primers, to the boiled colonies. It was assumed that the annealing temperature difference would not affect the 16S primer mix drastically, and so the protocol under method 5 was implemented.

(Note: The second trial using 2ul each of the forward and reverse primer and the additional trial using 4ul of the 16S primer mix were loaded onto the same gel)

3.2.2 *E. coli* standardized controls

Ran five trials using the *E. coli* safe relative with different thermocycling conditions similar to those conducted for the PCR and gel electrophoresis of 19-6. All five trials began with boiling five samples of *E. coli* with 30 ul of sterile water; after boiling each sample for 10 minutes, the samples were placed in an ice bath for 10 minutes. This boiling/freezing step was repeated for a second interval. Each boiled sample ran under different PCR thermocycling conditions:

1. 11ul of boiled solution was added to 4ul of the 16S primer mix (1492R and 27FSSU, with a concentration of 4uM). Ran solution in thermocycler with the LAJ Program conditions.
2. 11ul of boiled solution was added to 4ul of the 16S primer mix (1492R and 27FSSU, with a concentration of 4uM). Ran solution in thermocycler with the LAJ 2 Program conditions.
3. 11ul of boiled solution was added to 1ul of a forward and 1ul of a reverse 16S primer (each at 5uM). Ran solution in thermocycler with the LAJ 3 Program conditions.
4. 11ul of boiled solution was added to 2ul of a forward and 2ul of a reverse 16S primer (each at 5uM). Ran solution in thermocycler with the LAJ 3 Program conditions.
5. 11ul of boiled solution was added to 4ul of the 16S primer mix (1492R and 27FSSU, with a concentration of 4uM). Ran solution in thermocycler with the LAJ 3 Program conditions.

These PCR products were then loaded onto a gel (made from 1g agarose gel and 100ml 1x TAE, with added 1ul of dye). 10ul of these PCR products were loaded left to right (1 through 4, respectively), and 5ul of a hyper ladder was added to the leftmost well for comparison. The gel ran at 110 volts for 1 hour.

(Note: the last PCR product under condition 5 was loaded onto a separate gel along with the genomic DNA extraction)

3.2.3 Genomic DNA extraction and sequencing

This procedure was taken from the Promega Corporation's Wizard Genomic DNA Purification Kit

Added 1ml of liquid culture to a 1.5ml microcentrifuge tube and centrifuged at 13,000-16,000 x g for 2 minutes in order to pellet the cells. After pellets formed, removed the supernatant. Added 600ul of Nuclei Lysis Solution and gently pipetted the solution until the cells became suspended in solution. Incubated at 80°C for 5 minutes to lyse the cells, afterwards cooled to room temperature. Added 3ul of RNase Solution to the cell lysate and inverted the tube 5 times to mix the solution. Incubated at 37°C for 30 minutes, and then cooled the sample to room temperature. Added 200ul of Protein Precipitation Solution to the RNase-treated cell lysate, and vortexed the mixture at a high speed for 20 seconds. Incubated the sample on ice for 5

minutes. Centrifuged the sample again at 13,000-16,000 x g for 3 minutes. Transferred the supernatant with the DNA to a new 1.5ml microcentrifuge tube containing 600ul of room temperature isopropanol.

(Note: Some supernatant may remain in the original tube containing the protein pellet. Leave this liquid in the tube to avoid contaminating the DNA solution with the precipitated protein.)

Gently mixed the solution by inverting the until the thread-like strands of DNA form a visible mass. Centrifuge at 13,000-16,000 x g for 2 minutes; then carefully aspirate the ethanol. Drained the tube onto a clean absorbent paper and allowed the pellet to air-dry for 15 minutes. Added 100ul of DNA Rehydration Solution to the tube and rehydrated the DNA by incubating it at 65℃ for one hour. During this process, periodically mixed the solution by gently tapping the tube. Then rehydrated the DNA by incubating the solution overnight at room temperature. Stored DNA at 4℃.

This extraction was put through PCR using the conditions under LAJ 3 and placed on a gel for electrophoresis with the condition 5 control (as aforementioned in section 3.2.2).

3.3 Isolate the Antibiotic Produced by 19-6

3.3.1 Organic extraction

Inoculated two PDA plates with 100ul of isolate 19-6 each, and incubated plates at 37℃ for two days. Used micro spatula to cut the plate in 1cm squares. Transferred squares into two separate 100mL conical test tubes. Pushed gel to the bottom of the bottle with micro spatula. Placed tubes in a -83℃ freezer for two days.

Removed the tubes from the freezer and transferred them to a 50℃-hot bath for 30 minutes. Then proceeded with extractions using two different organic solvents: ethyl acetate and methanol. For the ethyl acetate extraction, we took one of the test tubes and added 12 ml of ethyl acetate and 8 ml of water. For the methanol extraction, we added 12 ml of methanol to the other test tube. Capped the test tubes and placed them onto a rocker at room temperature overnight.

3.3.2 High pressure liquid chromatography

Using the Agilent 1000 series HPLC equipped with a DAD 1 UV-Visible lamp, and Zorbax Rx-C18 column, prepared to purify the antibiotic producing agent from the organic extractions (Ball and Royer, 2019). First, washed the columns with 100% acetonitrile to prevent cross-contamination. Then placed 30ul of each organic extraction into different HPLC vials until no liquid remained above the agar in the conical tubes. Placed tubes in the HPLC machine. Used the protocol programmed by Richard Wobbe seen in the table below:

Table 3: HPLC Table

Time (min)	% Solvent A (0.1% formic acid in dH_2O)	% Solvent B (0.1% formic acid in acetonitrile)	Volume (mL)
0	92	8	
4.25	92	8	4.25
29.25	20	80	25
37.55	20	80	8.3
37.56	10	90	
45.85	10	90	8.3
45.86	92	8	
54.15	92	8	8.3

Program used to run organic extracts through (Wobbe, 2015).

3.4 Assess the Activity of the Isolated Antibiotic

Inoculated sterile filter paper disks with 15ul of the HPLC extracts (obtained from the second tube of each extract containing the peak observed from the DAD 1A UV-Visible lamp), numbered and labelled accordingly by their type of organic extraction. Sectioned 7 PDA and 7 LB plates for each fraction collected from the HPLC separation, and 2 blanks; labelled which ESKAPE safe relative would be spread. Spread 100ul of ESKAPE safe relatives (*B. subtilis, S. epidermidis, E. coli, A. baylyi, P. putida,* and *E. aerogenes)* and *M. smegmatis* onto their respective plates. Then placed the inoculated filter papers using sterile tweezers onto their designated section for each prepared plate. Incubated these plates at 37℃ for two days. Below is a schematic for the sections on each plate.

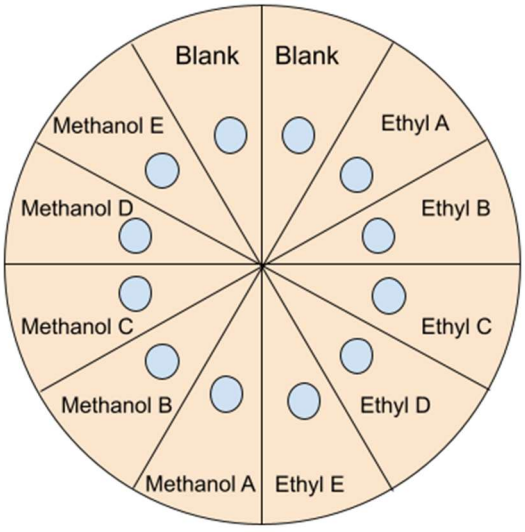

Figure 11: A schematic for the sections on each plate to test the strength of the isolated antibiotic from 19-6 against various ESKAPE safe relatives and M. smegmatis.

A second trial was conducted using the same procedure, albeit transferring 30ul each from tubes 2 and 3 of every fraction (meaning the apex and the falling slope observed from the

DAD 1 UV-Visible lamp) and vortexing these new fractions. From this mixture, we transferred 15 ul of these fractions onto filter papers and continued the procedure as previously stated.

Section 4: Results and Discussion

The following section includes our results in conjunction with our troubleshooting and future improvements of the methods performed. Our results were impacted by restricted laboratory access throughout the academic year along with limited resources beyond our lab space and the institution's COVID guidelines put in place. We believe that in a typical school year, our team would have had more communication with our advisors, access to more resources on campus, and an easier mailing system for the sequencing of different samples.

4.1 Test the Effectiveness of 19-6 Against Other Strains of Bacteria

4.1.1 Plate selected isolates on preferred media types

The different isolates for past years grew successfully on their preferred media types. These plates were then used to evaluate their ability to grow in the presence of the 19-6 isolate. Figure 12 displays the growth of each isolate grouped by their respective years.

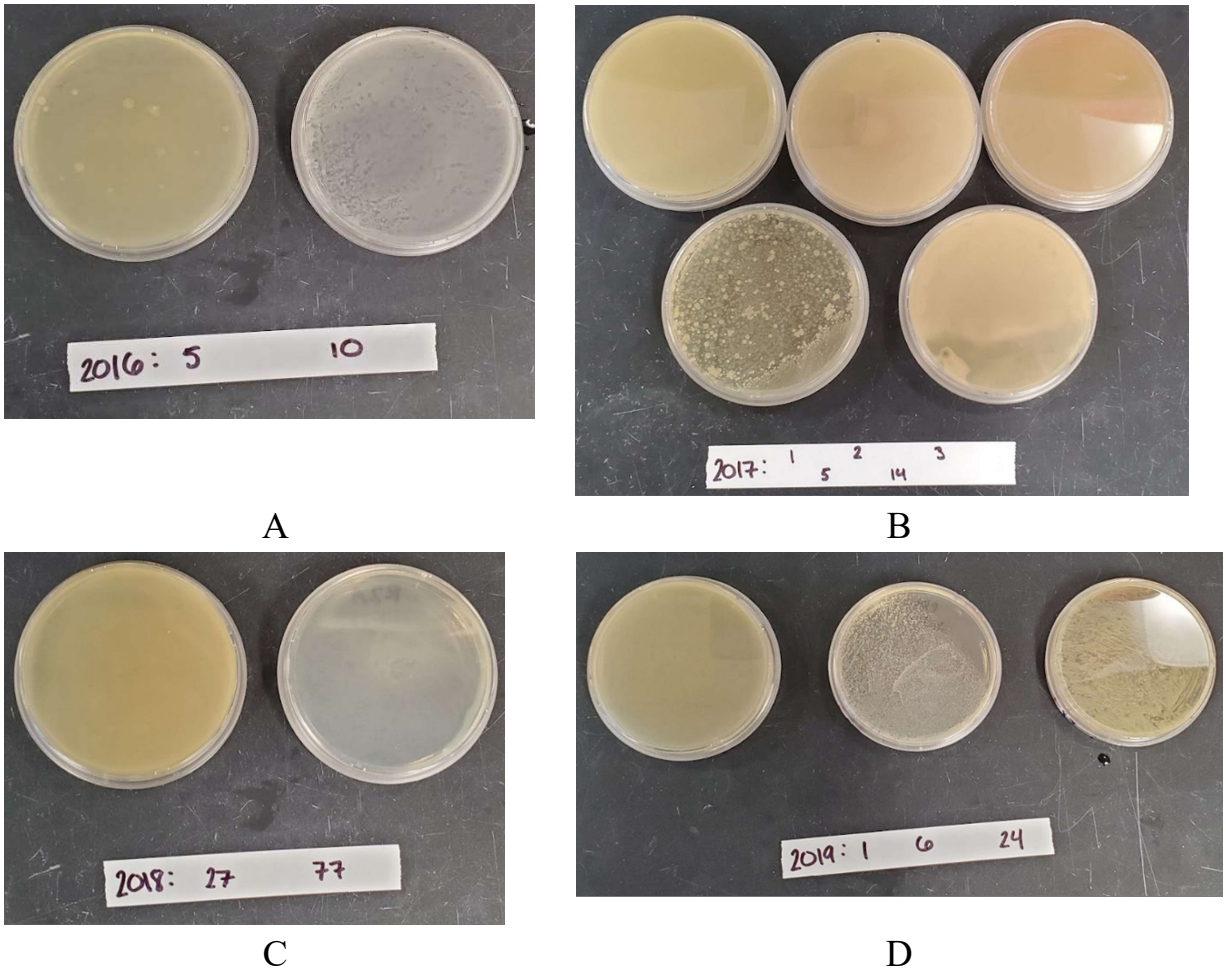

Figure 12: Each isolate from the previous years, when grown in their proper conditions on their preferred media, were able to survive and reproduce into more colonies. Images are labeled A through D in chronological order of isolation year, 2016 through 2019, respectively.

4.1.2 Plated 19-6 against past years isolates

Patch/Patch

19-6 was unable to inhibit the growth of the other isolates from previous years via the patch/patch procedure. As seen in figure 13, the growth of each isolate from past years were unhindered despite 19-6's presence. This could have been due to the fact that the patch/patch method does not allow the two different isolates to grow in concert; instead, they each grow independently, making it difficult to distinguish if any growth was stunted due to the presence of an antibiotic material. Another issue could possibly be that transferring on a smaller concentration of 19-6 onto a plate with full growth of a different isolate resulted in a lower production of the proposed antibiotic; that was then unable to affect the large presence of the opposing bacteria. Furthermore, we speculated that having the same plate incubated for such an extended period of time might have dried out the plate's media and prevented further growth of isolate.

Figure 13: No inhibition of the isolates from 2018 was seen in the presence of 19-6.

Spread/Patch

There did not appear to be any growth present on plates 2017-1, 2017-2, 2017-3, or 2017-14 after performing the spread/patch procedure, as shown in figure 14 below. This was not to be expected as we had hypothesized some growth would occur given the correct media types (in this case, TSA for 2017-1 ,2017-2, 2017-3, and 2017-14, as well as LB for 2017-5) for the previous years' isolates. We did have concerns knowing that 19-6 did not thrive under TSA media conditions, but to see that no growth has occurred on these plates suggests the possibility that 19-6 was present in some degree to inhibit nearly all the growth of the other isolates. This seems unlikely given the nature of these isolates and how they thrive under these conditions. Another possibility could be that although the previous years' isolates were able to grow independently on these media types, possibly with the presence of 19-6, these isolates are unable to grow to the same extent.

On the other hand, 2017-5 did show some growth, although no clear signs of inhibition. Here, it is known that 19-6 does not grow properly on LB media, so it is suggested here that the isolate from 2017-5 is able to grow because no 19-6 is present for competition, not due to the production of an antibiotic.

Figure 14: Spread/Patch results for the 2017 isolates; no growth appeared for isolates 1,2,5, or 14 in the presence of 19-6 on TSA, whereas 2017-5 did experience some growth on LB media.

Each previous year's isolate had then been grown on PDA (the preferred media of 19-6) using the spread/patch method. This yielded different results; as seen in the year 2017, no inhibition was visible on 2017-1, 2017-2, or 2017-3, this is likely because 19-6 was unable to produce an antibiotic that inhibits the growth of these isolates. As opposed to the TSA plates, we know that 19-6 grows well on PDA, so seeing this growth pattern of the 2017 isolates indicates that the 2017 isolates were able to resist any antibiotic that had been potentially released by 19-6, or that they were better able to out-compete 19-6. This also shows the possibility that the difference in media types affects the growth rate of each isolate growing in concert. There was clear inhibition seen in 2017-14 and both the isolates from 2016, as seen in the figure 15 below. On each of these plates, clear zones of inhibition have formed around the 19-6 isolate, effectively preventing the growth of the surrounding isolate. There is a possibility that the zone is caused by over-competition or a depletion of resources in these areas, however, the distinct rings suggest otherwise; and it has been determined that 19-6 was able to successfully inhibit the growth of these isolates through some production of an antibiotic. Furthermore, 2017-5 did not appear to have any significant growth in the presence of 19-6; although this was reasoned to be the results of 2017-5 being unable to grow on PDA, rather than any contribution of potential antibiotics from 19-6.

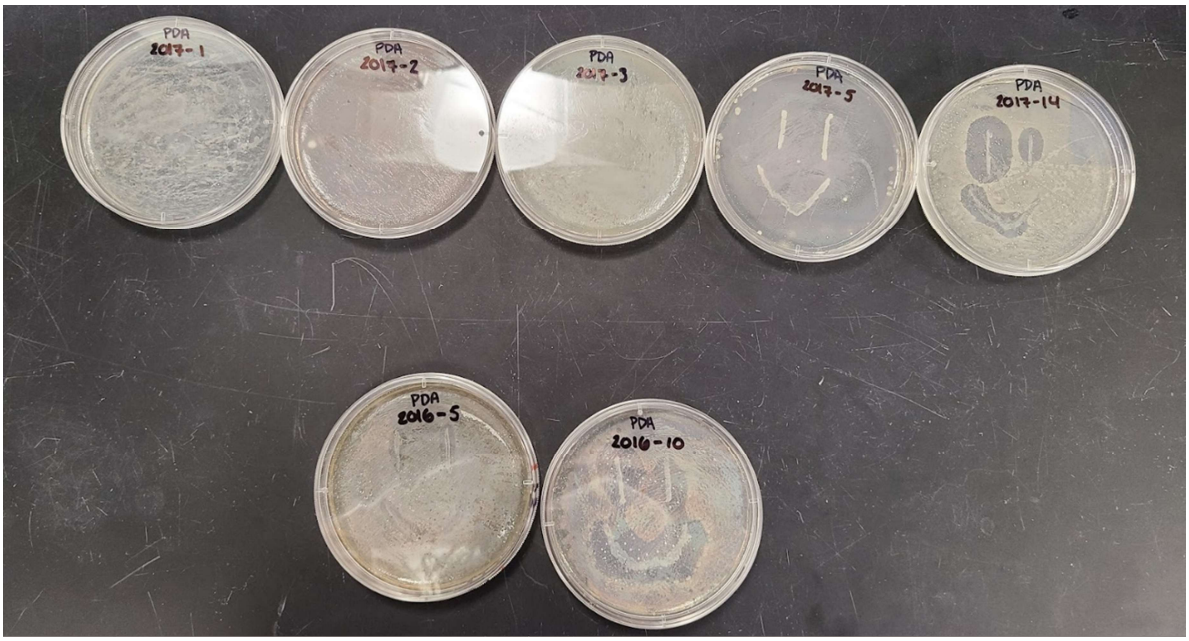

Figure 15: Spread/Patch results for the 2017 and 2016 isolates on PDA media; the only significant signs of inhibition occurred on 2017-14 and both isolates from 2016. The other 2017 isolates were able to grow without any signs of inhibition, with the exception of 2017-5 which showed no signs of growth.

Below in figure 16 are the plates from 2018 and 2019. Although 2018-77 and 2019-24 showed potential for signs of zones of inhibition, this distinction was determined to be caused by overcrowding and competition that results in a depletion of resources from the media. This would then cause the faint lines seen between the 2018/2019 isolates and 19-6. As for 2019-1, potential inhibition due to an antibiotic from 19-6 was proposed given clear signs of growth for 2019-1 present around the edges of the plate. It was because of this growth that our group decided 19-6 could be producing an antibiotic to inhibit the growth of the 2019 isolate. However, the large area of no growth surrounding 19-6 suggests other factors are in play to cause this growth pattern. Other factors could include similar ones aforementioned (i.e., competition and a depletion of nutrients).

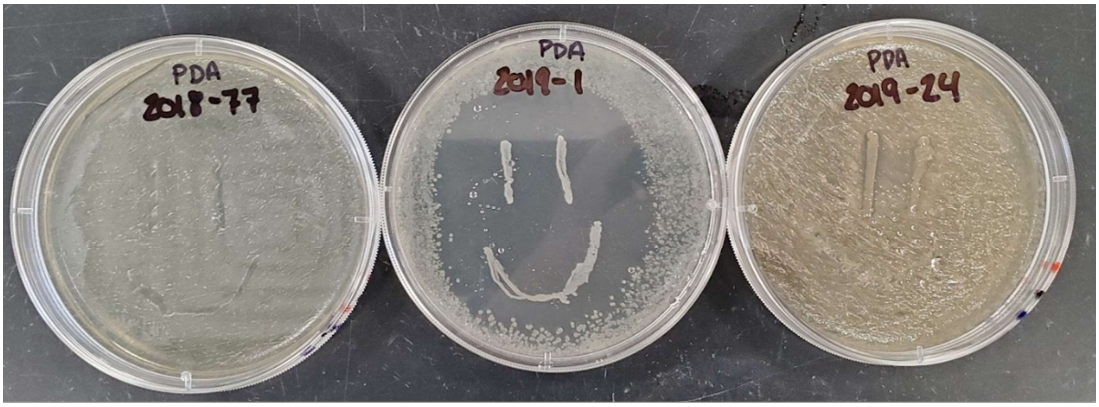

Figure 16: Spread/Patch results for the 2018 and 2019 isolates on PDA media; possible signs of inhibition appeared on 2018-17 and 2019-24, although this was suspected to be caused by other factors. 2019-1 was likely caused by a combination of similar factors and the potential production of a 19-6 antibiotic.

4.1.3 Plated 19-6 against ESKAPE safe relatives and *M. smegmatis*

The ESKAPE safe relatives and other safe pathogens were largely unaffected by the antibiotic, with the notable exception of *Mycobacterium Smegmatis*. Multiple trials were conducted using different media (either LB or PDA) and positive control groups for each ESKAPE safe relative and *M. smegmatis*. Both trials with the LB media held similar results, showcasing that selected ESKAPE safe relatives and *M. smegmatis* were able to grow on this media. The positive controls were labeled with their designated numbers (refer to table 1) and the letter C for control (e.g., 2C correlates to the positive control of *B. subtilis*). For trial 1, *M. smegmatis,* and *P. putida* were the only known safe pathogens to show any sort of inhibition in the presence of 19-6. Most notably *M. smegmatis,* as seen in figure 17, where a distinct zone of inhibition surrounded the 19-6 isolate against *M. smegmatis*. This highlights the possibility of an antibiotic producing factor in 19-6 that was able to prevent the growth of the surrounding *M. smegmatis. P. putida* also showed some forms of inhibition; however, these zones of inhibition were not as distinct or clear as for *M. smegmatis* and are more likely caused by other factors such as competition or a favor toward a specific type of nutrients (figure 17). Given this, we determined that *M. smegmatis* was the major safe pathogen that could be associated with inhibition for 19-6.

On the other hand, other ESKAPE safe relatives grew without any hindrance in the presence of 19-6 and covered the plates uniformly with growth. This brings up the possibility that 19-6 is not producing any antibiotic. However, the zone of inhibition seen in *M. smegmatis,* leaves the possibility that there is an antibiotic from 19-6, and that it simply does not affect the growth of certain ESKAPE safe relatives. With the latter, it is possible that 19-6 has the capability to inhibit the growth of a select few types of bacteria strains.

A B

Figure 17: Trial 1 of ESKAPE safe relatives, and M. smegmatis *test of inhibition in the presence of 19-6 on LB media. The most notable plates that did not show a complete overgrowth of the ESKAPE safe relatives in the presence of 19-6 are shown above;* M. smegmatis *(A), and* P. putida. *(B).* M. smegmatis *was the only safe pathogen to show a clear zone of inhibition, while* P. putida *had abnormal growth pattern with the growth only around the edges of the plate.*

A second trial was conducted of the same procedure and yielded similar results. *M. smegmatis* still showed promise towards the presence of an antibiotic factor inhibiting the growth of this safe relative, as seen in figure 20. This zone of inhibition is less clear than the first trial, but still more noticeable than the ESKAPE safe relatives which did not show any signs of inhibited growth on the designated plates. This was similar to the first trial; however, we did want to mention that we ran out of resources for *P. putida* to run a second trial on the LB media.

Also included in figures 18-20, are positive controls for some of the ESKAPE safe relatives and *M. smegmatis*, to show that if any inhibition had taken place, it was mostly likely caused by an antibiotic inhibiting its growth and not bacterial competition of resources, or a poor media preference by the safe relative. (Again, *P. putida* was discounted from this control group, which leads to uncertainty to why it had a peculiar growth pattern as aforementioned in trial 1).

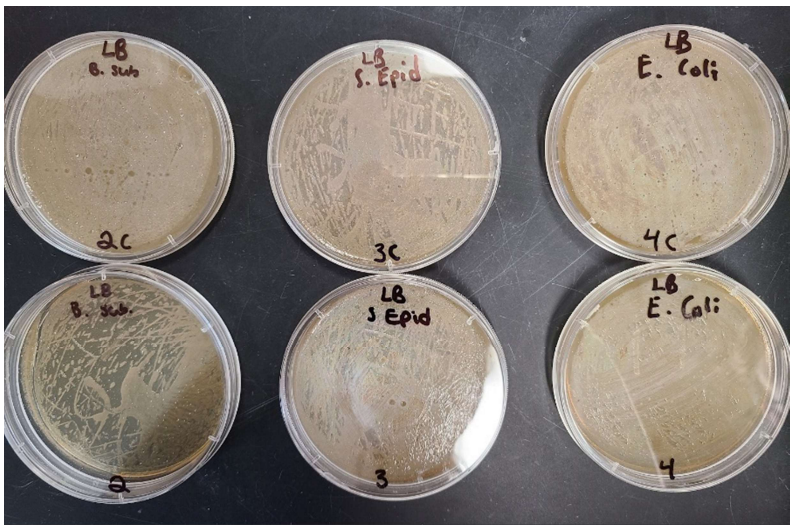

Figure 18: Trial 2 of ESKAPE safe relatives test of inhibition in the presence of 19-6 on LB media. Those shown are B. subtilis, S. epidermidis, *and* E. coli *(left to right), which all grew without any hindrance in the presence of 19-6. The controls for the LB trials (top) show that each ESKAPE safe relative present was able to grow on the LB media, so any lack of growth would be the result of inhibition by 19-6.*

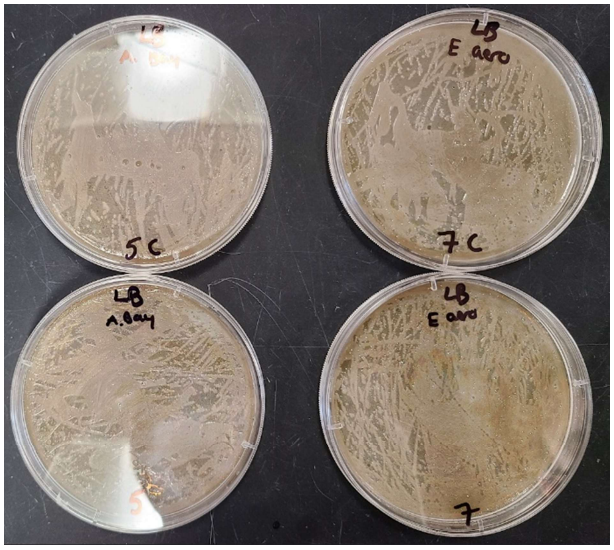

Figure 19: Trial 2 of ESKAPE safe relatives test of inhibition in the presence of 19-6 on LB media. Those shown are A. baylyi *and* E. aerogenes *(left to right) which all grew without any hindrance in the presence of 19-6. The controls for the LB trials (top) show that each ESKAPE safe relative present was able to grow on the LB media, so any lack of growth would be the result of inhibition by 19-6.*

Figure 20: Trial 2 of the M. smegmatis *test of inhibition in the presence of 19-6 on LB media.* M. smegmatis *shows clear signs of inhibition as in trial 1, designated by the red arrows. The control shows that* M. smegmatis *is able to grow on the LB media, so any lack of growth would be the result of inhibition by 19-6.*

We performed two more trials of the same procedure using PDA media. This was the preferred nutrient agar that 19-6 was able to grow on, and so we wanted to see its inhibitory activity when grown on its favored media type. The reason for conducting this experiment on LB media at all, was because most ESKAPE safe relatives, along with *M. smegmatis*, prefer LB media over PDA. This is most notable for *Pseudomonas Putida* which did not grow at all and yielded inconclusive growth as a result.

Similar to the LB trials, this experiment was done in duplicate on PDA plates using positive controls to ensure that the ESKAPE safe relatives and *M. smegmatis* would be able to grow on this media without the presence of 19-6; ensuring that any disruption of growth was

caused by the presence of 19-6. Also similar to the LB trials, the only notable inhibition appeared for *M. smegmatis* in both trials, as seen in figure 21.

Figure 21: Trial 1 of the M. smegmatis *to its test of inhibition in the presence of 19-6 on PDA media.* M. smegmatis *shows clear signs of inhibition as in trial 1, designated by the red arrows. The control shows that* M. smegmatis *is able to grow on the PDA media, so any lack of growth would be the result of inhibition by 19-6.*

Most of the ESKAPE safe relatives were able to grow without hindrance in the presence of 19-6 as they had in the LB trials, completely covering the plate with growth, as seen in figure 22. Unlike the LB trials, the *P. putida* safe relative did not grow on the PDA media, as seen in figure 23; therefore, any growth on these plates were strictly 19-6 and the inhibition was caused by the lack of proper nutrients, not by the presence of 19-6 or its proposed antibiotic.

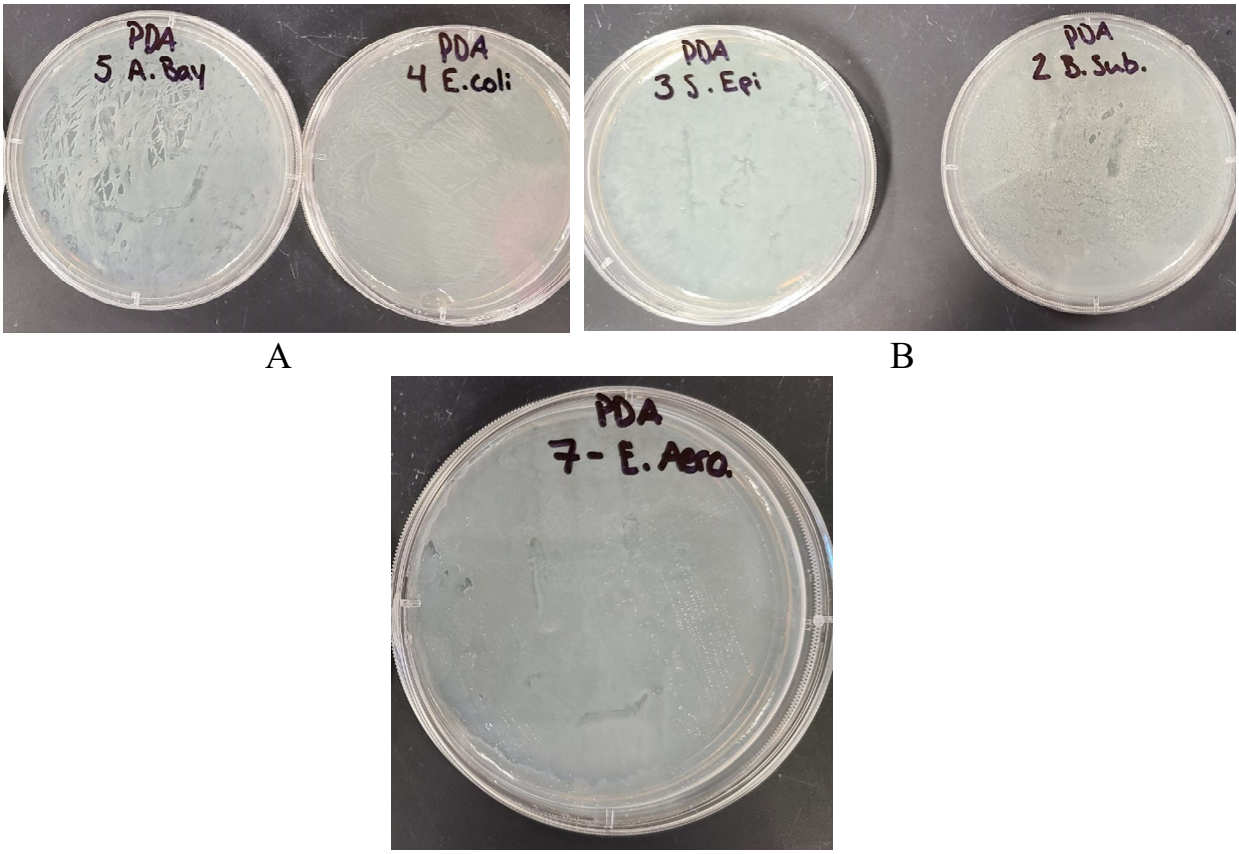

A B C

Figure 22: Trial 1 of ESKAPE safe relatives test of inhibition in the presence of 19-6 on PDA media. Those shown are S. epidermidis, B. subtilis, A. baylyi, E. coli, *and* E. aerogenes *(A, B and C respectively) which all grew without any hindrance in the presence of 19-6.*

Figure 23: Trial 1 of P. putida *was unable to grow on PDA media as seen above (right), where a plate inoculated with the safe relative shows no growth without the presence of 19-6. On the left, only 19-6 is*

grown/visible, while P. putida *still shows no growth with or without the presence of 19-6. This is likely caused by improper nutrients provided by the media considering the control plate (left).*

A second trial was conducted on PDA media using the same procedure and yielded similar results. Positive controls for some of the ESKAPE safe relatives and *M. smegmatis* were used to show that if any inhibition had taken place, it was mostly likely caused by an antibiotic inhibiting its growth and not bacterial competition of resources, or a poor media preference by the safe relative.

M. smegmatis still showed promise towards the presence of an antibiotic factor inhibiting the growth of this safe relative, as seen in figure 24.

Figure 24: Trial 2 of the M. smegmatis *to its test of inhibition in the presence of 19-6 on PDA media.* M. smegmatis *shows clear signs of inhibition as in trial 1, designated by the red arrows. The control shows that* M. smegmatis *is able to grow on the PDA media, so any lack of growth would be the result of inhibition by 19-6.*

This zone of inhibition for *M. smegmatis* is less clear than the first trial, but still more noticeable than the ESKAPE safe relatives which did not show any signs of inhibited growth on the designated plates. This was similar to the first trial, and once again *P. putida* showed no growth due to insufficient nutrients provided by the PDA media, as seen in the figure below.

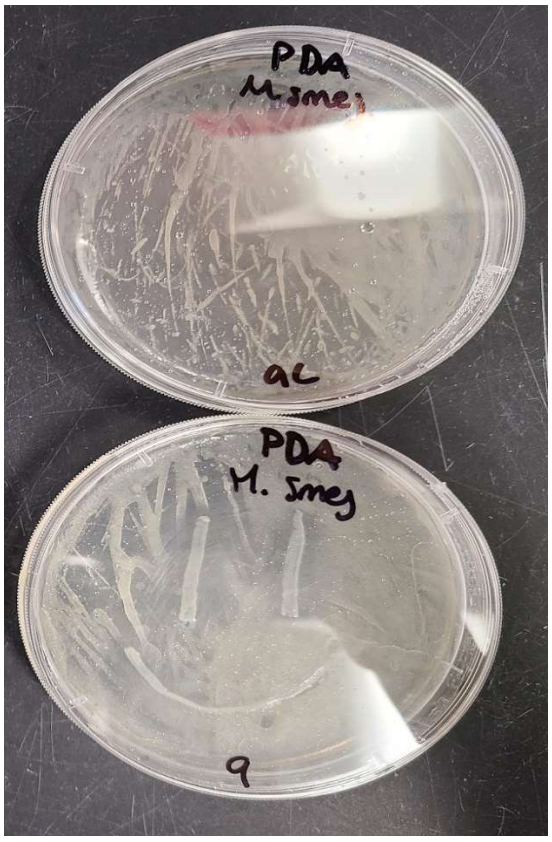

Figure 24: Trial 2 of the M. smegmatis *to its test of inhibition in the presence of 19-6 on PDA media.* M. smegmatis *shows clear signs of inhibition as in trial 1, designated by the red arrows. The control shows that* M. smegmatis *is able to grow on the PDA media, so any lack of growth would be the result of inhibition by 19-6.*

This zone of inhibition for *M. smegmatis* is less clear than the first trial, but still more noticeable than the ESKAPE safe relatives which did not show any signs of inhibited growth on the designated plates. This was similar to the first trial, and once again *P. putida* showed no growth due to insufficient nutrients provided by the PDA media, as seen in the figure below.

Figure 25: Trial 2 P. putida *was unable to grow on PDA media as seen in the control (top), where a plate inoculated with the safe relative shows no growth without the presence of 19-6. On the bottom, only 19-6 is grown/visible, while* P. putida *still shows no growth with or without the presence of 19-6. This is likely caused by improper nutrients provided by the media considering the control plate.*

The other ESKAPE safe relatives were able to grow without hindrance in the presence of 19-6 as they had in the first trial using PDA media, and the LB trials. These strains completely covered the plate with growth, as seen in figure 26.

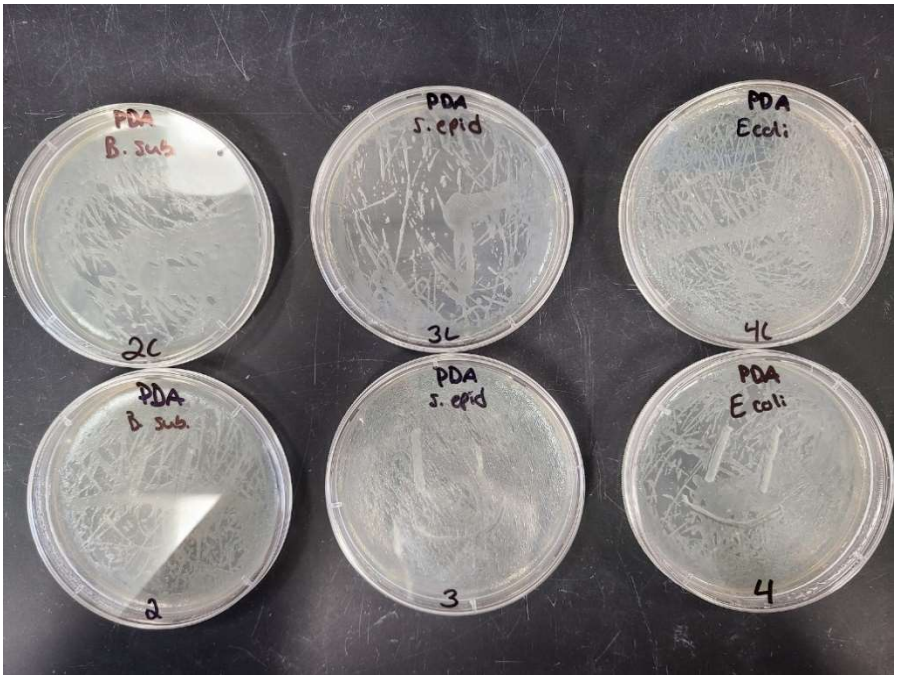

A

B

C

Figure 26: Trial 2 for PDA media, similar results to trial 1, those shown are B.subtilis, S. epidermidis, E. coli, E. aerogenes, *and* A.baylyi *(left to right) which were all able to grow on the PDA media, and experienced normal growth patterns when exposed to 19-6.*

The lack of inhibition in the other ESKAPE safe relative strains proposes the idea that no antibiotic is produced from 19-6. However, similar to the LB trials, because the zone of inhibition is seen against *M. smegmatis*, it is still a possibility that an antibiotic is being produced by 19-6. Moreover, as mentioned before, despite being unable to inhibit the growth of the ESKAPE safe relatives, this antibiotic may be able to inhibit the growth of a select few other bacteria stains. It was, therefore, concluded that only *M. smegmatis* was inhibited by 19-6 in all trials for both LB and PDA media, yielding the possibility of a functioning production of some antibiotic in this isolate.

In future attempts, it was decided that different media may impact the antibiotic yield, and to grow 19-6 on different media types (e.g., TSA, trypticase soy agar) to test against the ESKAPE safe relatives and *M. smegmatis*; along with testing 19-6 against more known bacterial strains to see its effectiveness over a more diverse sample size.

Additionally, our team would have preferred to restart our process from the beginning, starting with a new soil sample. It was theorized that the constant freezing and thawing of the 19-6 liquid culture over the course of our research could have altered the isolate's characteristics. Keeping in mind that this isolate was from 2019, it's possible that the antibiotic has lost function over the past few years, and in turn, greatly impacted its ability to inhibit different bacteria.

4.2 Identify the 16S Ribosomal Gene of 19-6

4.2.1 PCR and gel electrophoresis

The amplification of the rRNA 16S gene was meant to identify our isolate 19-6, in terms of its genus. The 16S rRNA gene is known as a universal indicator for most bacteria. The most common primers used to amplify the 16S region are the 27F and 1492R, and they were modeled from the 16S rRNA region of E. coli. Since the primer's creation over 25 years ago, there has been speculation about their ability to amplify all 16S regions using current replication methods (Frank et.al., 2008). Researchers have been testing both longer and shorter primers with slight alterations to the base pairs, in hopes to find a more conserved length within the 16S region. Though there is a possibility that our 19-6 isolate did not carry the 16S rRNA gene at all, it was deemed unlikely for our bacteria. However, over the course of the different methods employed for this sequencing procedure, our various attempts proved unsuccessful. Our methods most consistently resulted in the bands falling around 200 base pairs in comparison to the hyper ladder; and in some did not show on the gel at all. The 16S rRNA gene should have fallen around 1500 base pairs, so these short bands did not help in our identification of 19-6. Figures 27-30 display images of the bands under a UV lamp.

Figure 27: The bands resulting from method 1 of PCR amplification; no dye was added directly to the gel, resulting in faint bands in lanes 2 and 4, rendering our results for this method inconclusive. The ladder was not visible under UV; however, it was added to lane 1.

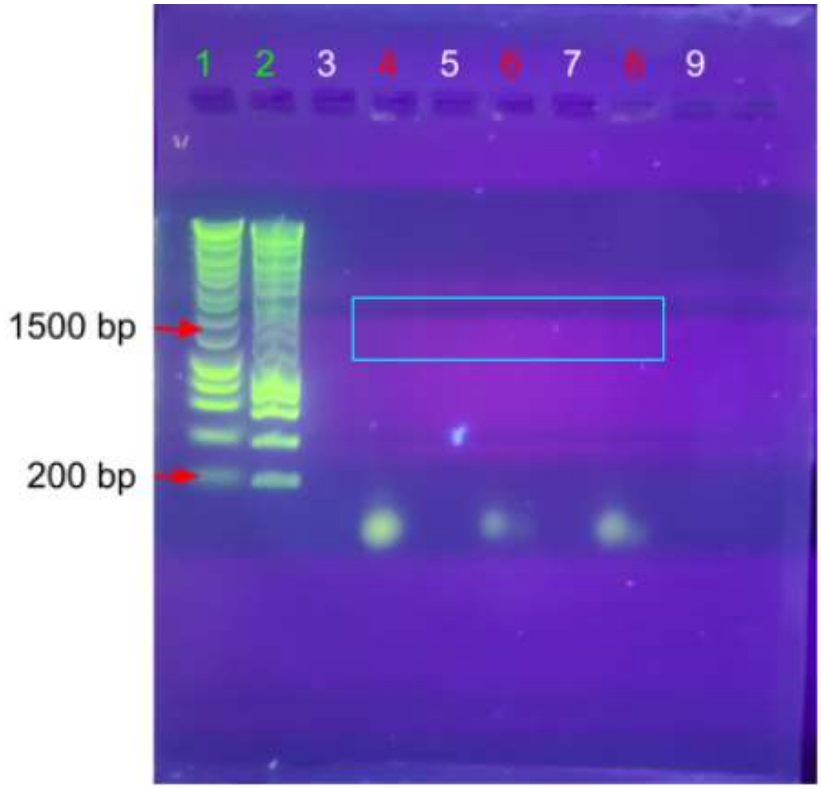

Figure 28: The bands resulting from method 2 (an identical procedure to method 1, albeit the addition of dye directly to the gel to help the bands fluoresce under UV light). Here, the bands were expected to fall within the light blue box, around the 1500bp band. However, samples in lanes 4, 6 and 8 all fall below the hyper ladder, registering at about 200bp.

This base pair value seen in method 1 and 2 does not align with that of the 16S rRNA gene and could not be used for sequencing the bacteria's DNA to properly identify its genus. It was speculated that the bands that appeared around 200bp may have been the 1xTaq dye itself or the primer used to amplify the gene sequence, instead of the 19-6 DNA. Meaning that either there had not been a sufficient amount of DNA that had been successfully separated by the gel electrophoresis, or that the amplification of the 16S rRNA gene was unsuccessful.

Method 3's bands, circled in figure 29, had fallen below the hyper ladder, identical to the previous gels, resting around 200bp. Method 4's bands did not appear on the gel (refer to figure 29). Similar to the previous methods, method 3's bands may have suffered the same errors in its procedure, and as for method 4, we concluded that the thermocycling conditions may not have completely denatured the bacteria, resulting in the DNA being unable to properly separate out in the gel.

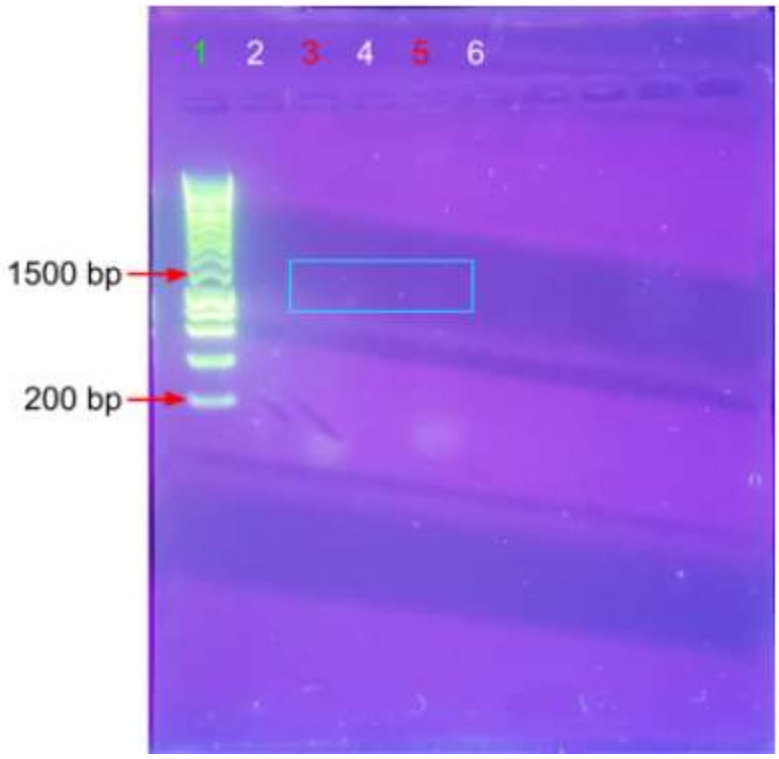

Figure 29: The bands above show the results from both methods 3 and 4 (lanes 3 and 5, respectively), which had different thermocycling conditions for their PCR amplification procedures. Faint bands can be seen below the 200bp band on the ladder in lane 1, when they were expected to be seen within the light blue box (around 1500bp).

The gel for method 5 (shown in figure 30) had no bands visible similar to method 4, resulting in our procedure rendered inconclusive for similar reasons involving the thermocycling conditions incompletely denaturing the bacteria, so that the DNA was unable to properly separate in the gel.

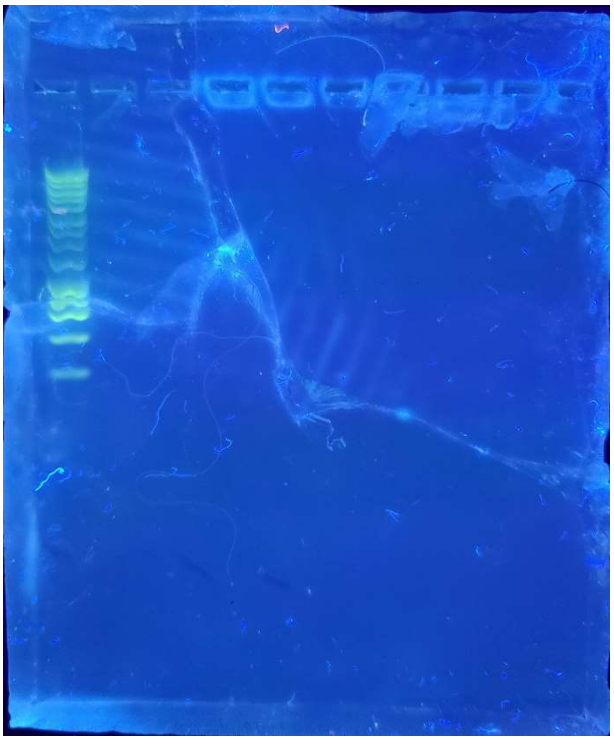

Figure 30: No bands appeared after the thermocycling conditions associated with method 5 for the PCR amplification of the 16S rRNA gene.

As for the second trial for method 5 that used 4ul of the primer mix instead of separate forward and reverse primers, the bands also did not appear on the gel. Again, this is likely caused by similar errors as found in methods 4 and 5 above.

Due to these inconclusive bands from the PRC products (along with trouble with the mailing system due to Covid), we were unable to excise and send the bands off for sequencing, and therefore also could not run a BLAST to compare the gene sequence to known bacteria for a proper identification of 19-6.

4.2.2 *E. coli* standardized controls

Using *E. coli* as a positive control, the 16S rRNA gene should have presented itself in bands around 1500bp of the hyper ladder. This would signify that the methods used for 19-6 were successful in separating DNA in an identified genus/species of bacteria, and that 19-6 either did not possess, or had a significantly lower amount of the 16S rRNA gene. However, the bands provided from the *E. coli* under the four different methods (given that the only difference between method 1 and method 2 was that the latter had the addition of dye to the gel itself) employed gave similar results to our 19-6 bands: method 1 (and method 2), method 3, and method 4's bands fell around 200 bp. The only significant difference in these results compared to 19-6 was that method 4's bands did appear for the *E. coli* sample, as seen in the figure below. Method 5's PCR products were run on a separate gel along with the extracts from the genomic extraction; both of which had bands that did not fluoresce under the UV light.

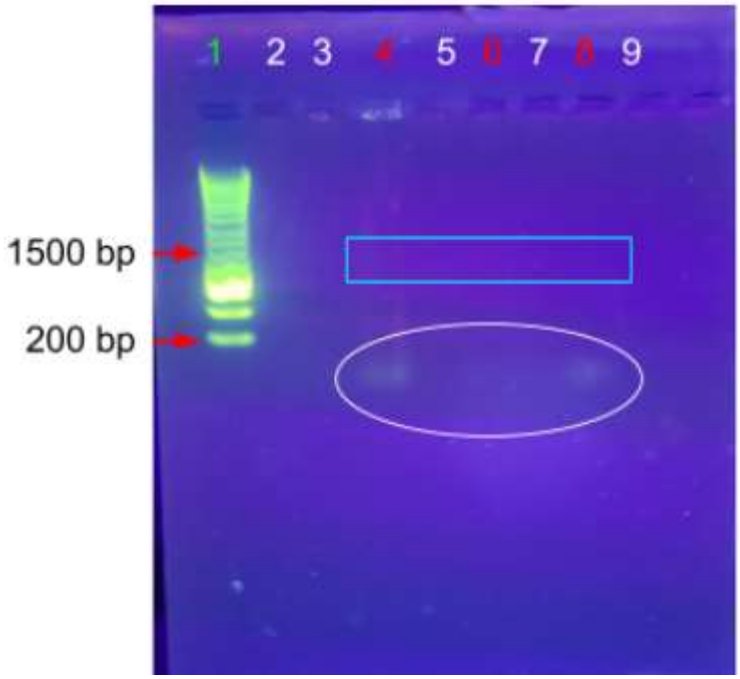

Figure 31: The E. coli bands after the PCR and gel electrophoresis procedures employed to 19-6. Bands from method 1 (and 2), 3, and 4 (lanes 4, 6 and 8 respectively) were visible. Method 5's PCR products were run on a gel with the genomic extraction's PCR products.

These results from the positive controls led us to new hypotheses for our research in the identification of 19-6. The *E. coli* control should have had bands that fell at 1500bp for the amplification of the desired gene, however, this was not the case using the different thermocycling conditions that have been used in previous research projects done by WPI students in Professor Buckholt's classes. Our group then decided that it could be an error in the instrumentation used for the procedures, or that the hyper ladder had not been a viable comparison to indicate the presence of the 16 rRNA gene. To ensure that we were able to successfully extract DNA from 19-6, in order to sequence and identify the bacteria, we performed a genomic DNA extraction.

4.2.3 Genomic DNA extraction and sequencing

The PCR products of the genomic extraction (along with the products from method 5's controls, as previously stated) did not produce visible bands on the gel after electrophoresis. This initially led us to believe we had not successfully extracted DNA from 19-6. However, the values for concentration obtained through the genomic DNA extractions were 11.8 ng/ul and 1.9 ng/ul, for separate trials. These extractions were unable to be mailed out for sequencing due to time constraints during the break between terms. These concentrations, however, are evidence that DNA was extracted from 19-6, and led to our two conclusions as to why our bands were unable to identify 19-6's genus. Knowing that there is DNA that was able to be extracted at this concentration, means that there should have been enough DNA to be separated out in the gel during electrophoresis, however, it is possible that that the amplification of the 16S rRNA gene

was unsuccessful, and therefore rendered our bands inconclusive. On the other hand, in light of our *E. coli* controls, it still remains a possibility that an error with the hyper ladder is the cause for a misinterpretation of the base pair measurements of the 19-6 bands in each of the methods.

We had decided that the PCR was less likely to be the source of error for this process because of how we varied the thermocycling conditions, particularly the annealing temperature along with the concentration of our isolate throughout multiple attempts. In this way, we had ruled out the possibility of the PCR amplification failing to replicate our gene sequence given so many variations that could have posed a problem during the replication process. On the other hand, our positive controls yielding similar results to our unknown 19-6 sample, led us to believe that PCR could still be an issue considering we should have seen those bands fall around 1500bp for one of these methods/conditions. However, the explanation concerning the hyper ladder could also atone for these inconclusive band lengths. It is possible that the hyper ladder was not being separated down the gel properly, rather it was falling short, instead of completing its separation. If this were the case, then our bands for 19-6 had been inaccurately measured, and could possibly be falling at 1500bp, despite where the hyper ladder ends, because the hyper ladder may not have separated completely to cover that 1500bp mark/length. Some of the procedures mentioned in the methods section involved varied voltages and run times for the gels to try and rule out the possibility that the hyper ladder was compromised; however as seen above and in the previous section, this was not the case and the bands still fell around 200 bp.

It is also a possibility that our isolate 19-6 simply does not encode for the 16S rRNA gene, although uncommon, this poses a definite stumbling block in our identification procedure. In further experimentation, it would have benefitted us to look at other common gene sequences that may help to identify our isolate in a similar fashion given the proper primers for these different genes that were unavailable to our group at this time. In future attempts, we would also like to obtain a new hyper ladder to identify this gene and continue with the different thermocycling procedures, in the efforts to isolate the bacterial DNA to sequence using the BLAST database. Additionally, we would have also preferred to send out our genomic extraction as well for sequencing. However, due to time constraints involving the COVID-19 restrictions on our lab time, our group made the decision with Professor Buckholt's guidance, to continue on with our research without the complete identification of 19-6.

4.3 Isolate the Antibiotic Produced by 19-6

4.3.1 Organic extraction

The organic extractions using methanol and ethyl acetate were successful in clear separations between the treated agar (previously inoculated with 19-6) and the organic solvent. The organic solvent contained the proposed antibiotic producing agent through the destruction of 19-6's bacterial cell walls. The methanol extraction had a less clear separation between the solvent and the agar compared to the ethyl acetate extraction, as shown below in figure 32. A possible reason for this could be the PDA media used instead of LB, which is commonly used for

these types of extractions. We decided to use PDA because 19-6 grows better on PDA, rather than LB, however, this could have caused poorer extractions by the organic solvents, particularly methanol.

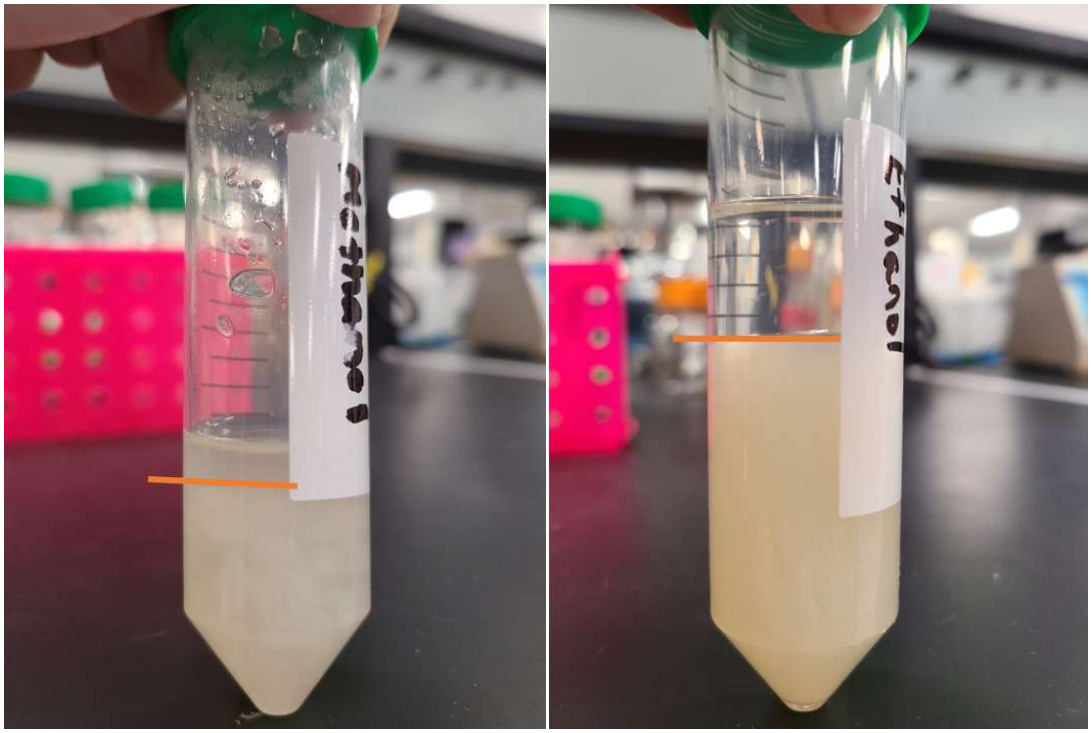

Figure 32: Separation after organic extraction by methanol (left) and ethyl acetate (right).

The liquid portion, designated in the red margins, above the agar contains methanol and ethyl acetate, respectively, along with the proposed antibiotic producing agent now isolated from 19-6. These organic extractions were unable to be tested alone against various ESKAPE safe relatives and *M. smegmatis* due to the potency of the organic solvents which damaged the plates on contact. In future attempts, we would have opted to allow the extracts time to evaporate off the organic solvents in a fume hood or use glass plates instead of plastic to prevent this damage. However, this set back and the heightened time restrictions toward the end of our term, did not allow us to test the effects of these extracts alone, and instead we carried on with the testing of the HPLC extracts from these organic solvents. A flow chart for the labelling and organization of the organic extracts to HPLC is displayed in the figures below.

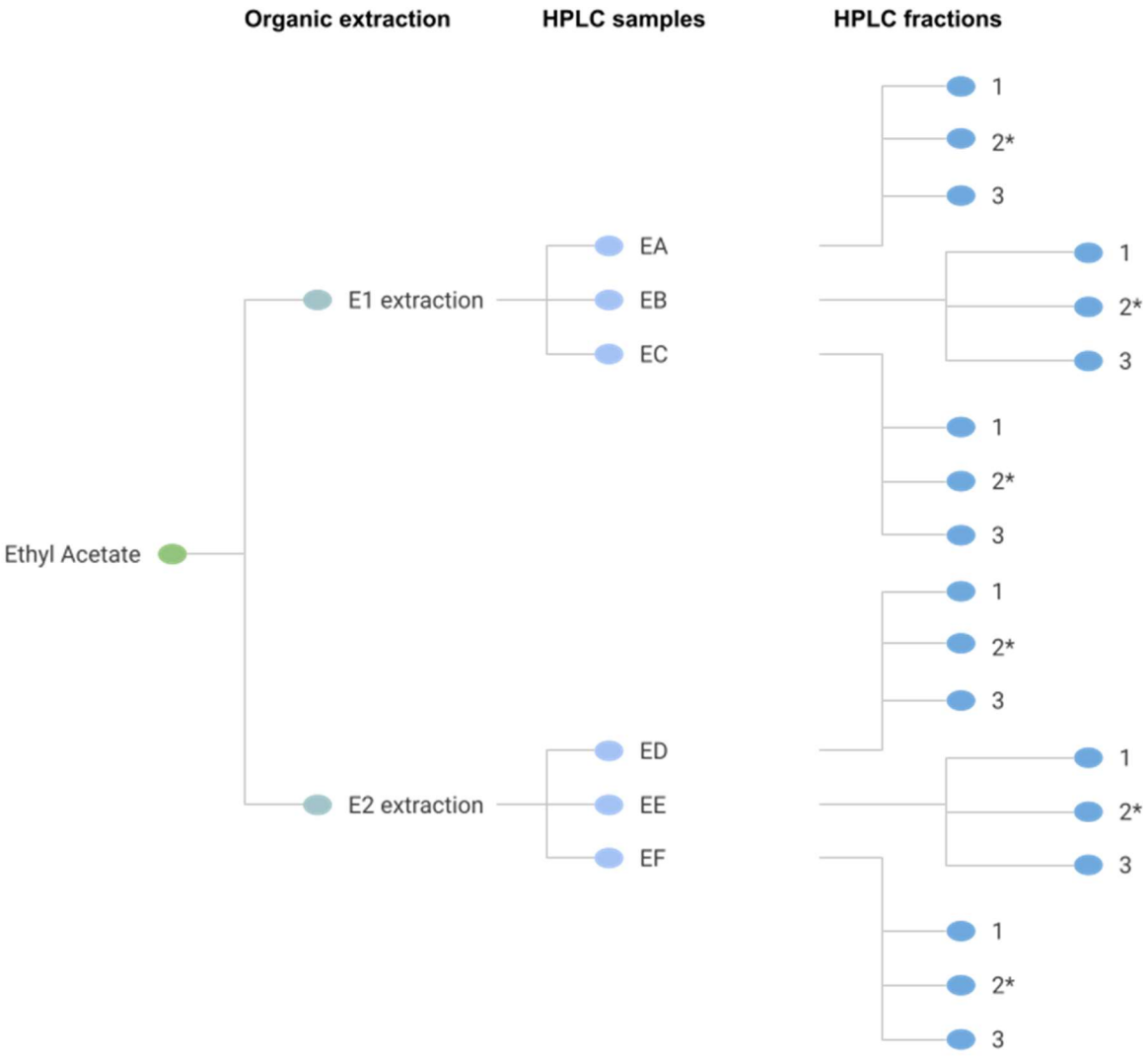

Figure 33: A flow chart of the organic extracts from the ethyl acetate solvent that were subjected to HPLC. The asterisks next to the number labels for the HPLC fractions designate the fractions that were used to observe the effectiveness of the purified antibiotic against ESKAPE safe relatives and M. smegmatis.

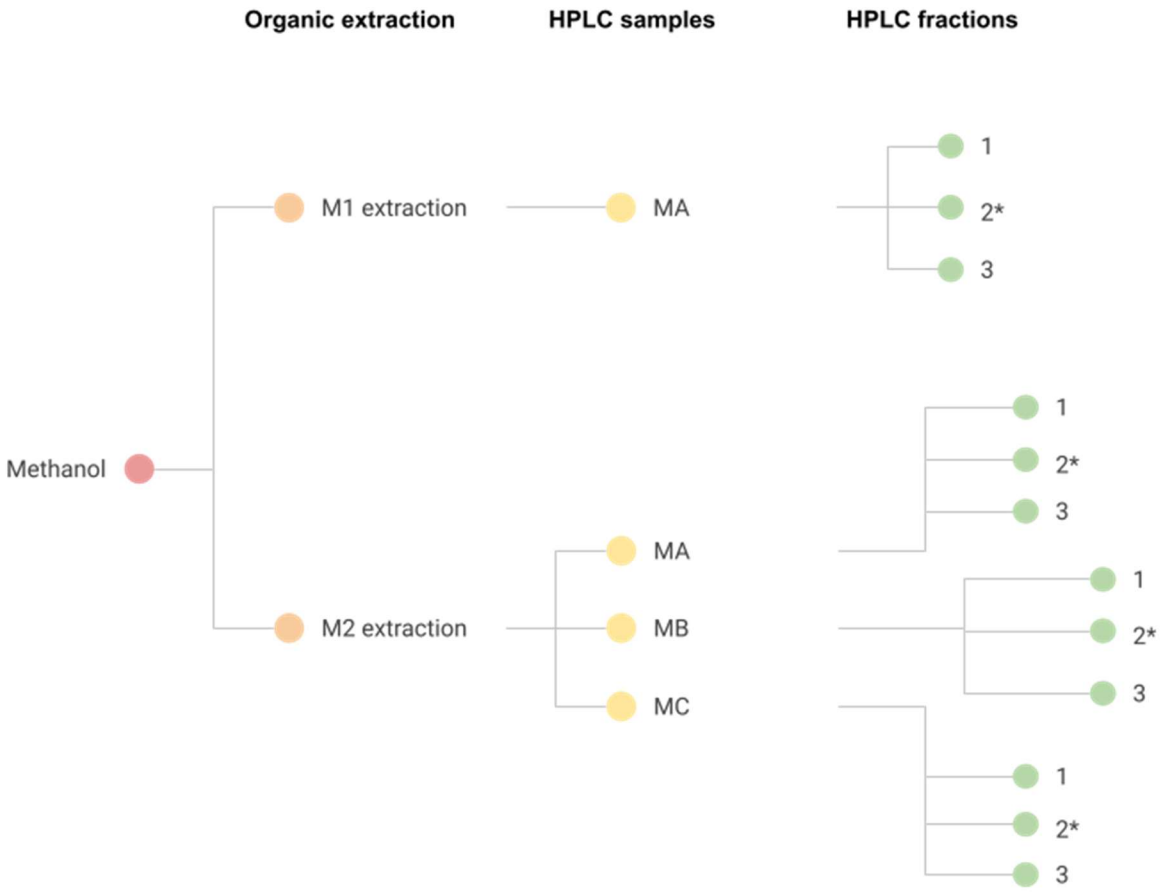

Figure 34: A flow chart of the organic extracts from the methanol solvent that were subjected to HPLC. The asterisks next to the number labels for the HPLC fractions designate the fractions that were used to observe the effectiveness of the purified antibiotic against ESKAPE safe relatives and M. smegmatis.

4.3.2 High pressure liquid chromatography

To further determine the identity of the antibiotic believed to be within the organic extractions, multiple samples were prepared for analysis using a standard HPLC setup. For each of the samples, the software used to run the system automatically calculates a purity analysis when the program stops or is ended by the user. The program favors the primary signal A, with a UV range around 246 nm, for most of the calculations and is therefore used for the peak analysis calculations throughout this report.

The first step in analyzing purity is done through the comparison of the spectra within the peak. The visualization of the comparison is found in the bottom left panel, see figure 35 below. On the contrary, when a peak is considered pure the spectra will be identical or very similar. For our program, up to 5 spectra from a peak are compared for calculations.

In order to have an accurate estimate of when to collect fractions from our samples, we initially ran control samples with the solution used for the organic extractions. A portion of the ethyl acetate control can be seen below in figure 35.

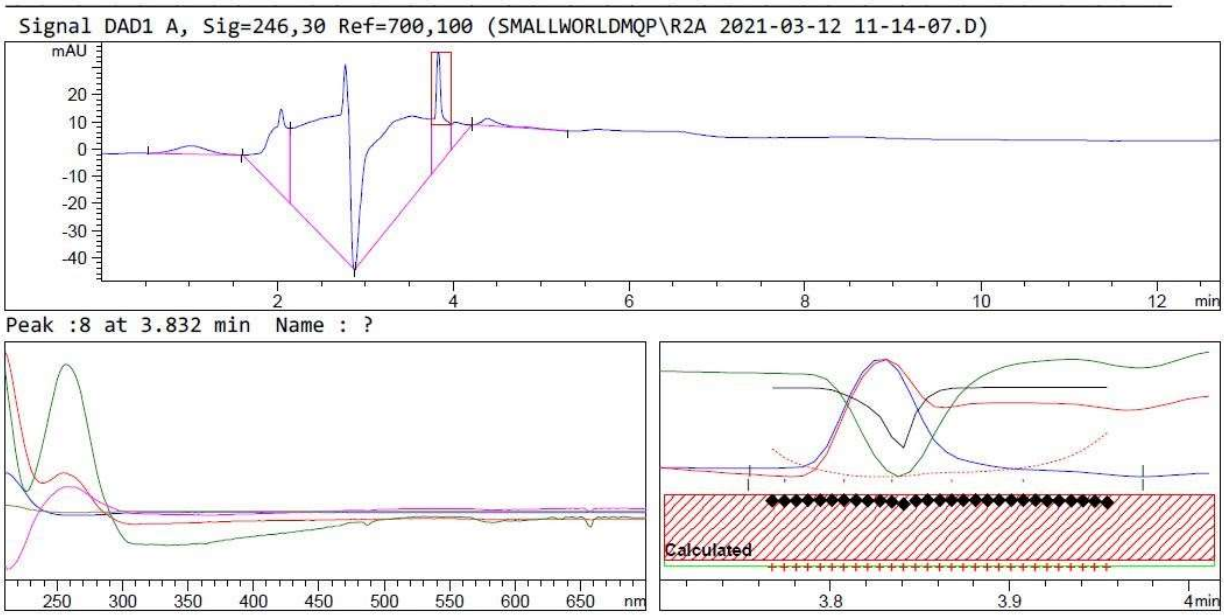


```
-> The purity factor exceeds the calculated threshold limit. <-

Purity factor : 232.919 (29 of 29 spectra exceed the calculated threshold limit.)
Threshold     : 996.897  (Calculated with 29 of 29 spectra)
Reference     : Peak start and end spectra (integrated) (3.754 / 3.974)
Spectra       : 5  (Selection automatic, 5)
Noise Threshol: 0.123  (12 spectra, St.Dev 0.0576 + 3 * 0.0219)
```

Figure 35: Ethyl acetate control sample, analyzed by the software automatically when the program completes or is ended by the user.

As shown in the top panel, a few peaks were recorded within the two- and four-minute time frame. This gave us a general idea of where peaks may appear that could be attributed to the solution of the sample, and not our antibiotic. Therefore, the fractions collected from our ethyl acetate samples were after the four-minute time frame and were presumed to have our antibiotic. In order to collect a majority of the peak, fractions were typically separated into three 0.5 mL Eppendorf tubes. The tubes would be collected corresponding to the upslope, apex, and downslope of the peak and labelled 1 through 3 respectively. Through both our first and second trials of ethyl acetate, each run showed a peak around the six-to-eight-minute time frame. This consistency led us to believe that our antibiotic may be eluted around this time frame.

In total, each ethyl acetate sample would take approximately 15 minutes to complete running. Once the run was completed, the analysis report was saved to a removable hard-drive and the next sample was prepared. In order to complete as many samples as possible, analysis reports were not inspected in full between runs. If they had been fully read through, we could have noticed that our collected peaks from each sample were exceeding the calculated threshold limit. Thus, meaning that none of our ethyl acetate samples could be considered pure. An example analysis report from the first ethyl acetate sample, Ethyl acetate A (EA), from trial one is shown in figure 36 below.

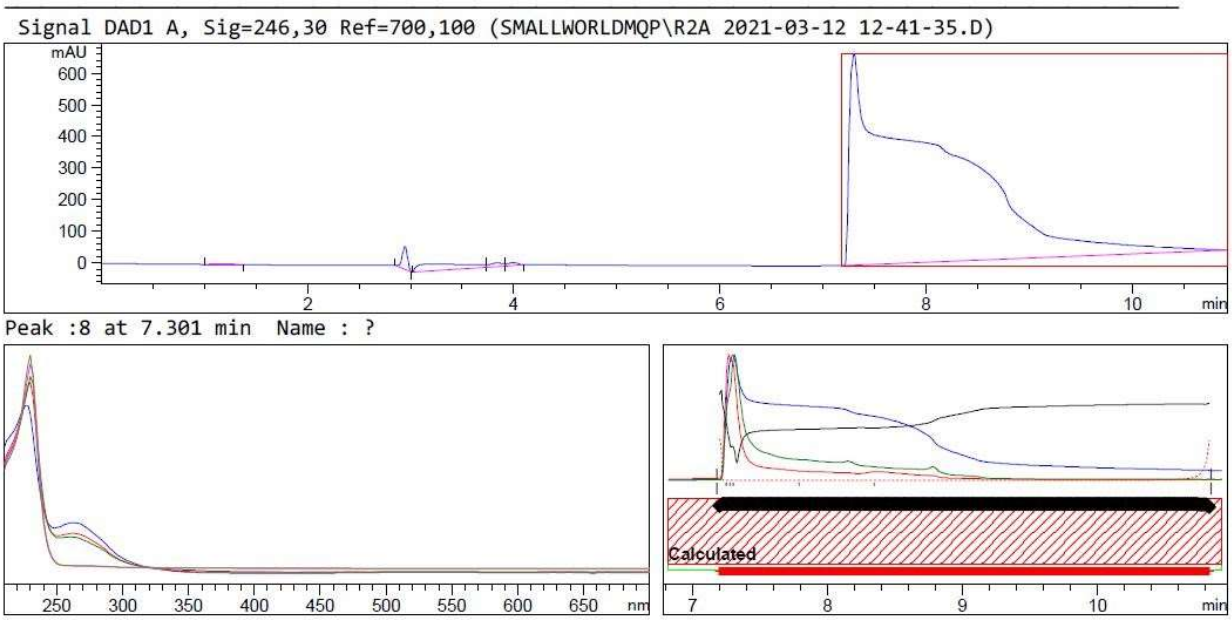


```
-> The purity factor exceeds the calculated threshold limit. <-

Purity factor : 882.142 (545 of 545 spectra exceed the calculated threshold limit.)
Threshold     : 999.895  (Calculated with 545 of 545 spectra)
Reference     : Peak start and end spectra (integrated) (7.181 / 10.841)
Spectra       : 5  (Selection automatic, 5)
Noise Threshol: 0.089  (12 spectra, St.Dev 0.0441 + 3 * 0.0149)
Warning       : Spectral absorbances > 1000 mAU (see help for more information)
```

Figure 36: Analysis report for the ethyl acetate sample labelled EA. An additional warning was also reported to indicate that there were spectral absorbances present affecting the reading of spectra and subsequent calculations.

Our methanol runs were relatively the same as the ethyl acetate runs. Figure 37, below, shows where a few peaks were recorded within the two- and five-minute time frame for the methanol control run. This gave us another general idea of where we may see peaks to attribute to methanol in our samples. However, the fractions collected from our methanol samples were also within the two- and four-minute time frame. Like before, fractions were typically separated into three 0.5 mL Eppendorf tubes following the shape of the peak and labeled accordingly. Through both our first and second trials of methanol, each run had a peak around the three-minute time frame. No peaks were seen after the five-minute point in each of the runs between the two trials.

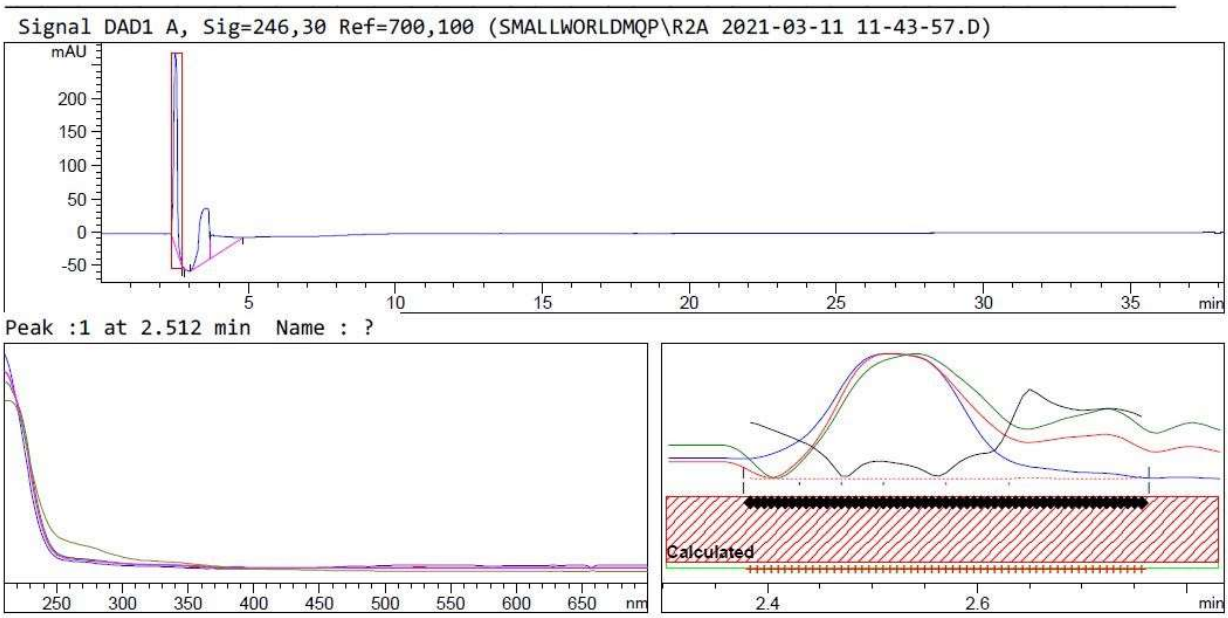


```
-> The purity factor exceeds the calculated threshold limit. <-

Purity factor : 894.431 (57 of 57 spectra exceed the calculated threshold limit.)
Threshold     : 999.992  (Calculated with 57 of 57 spectra)
Reference     : Peak start and end spectra (integrated) (2.377 / 2.764)
Spectra       : 5  (Selection automatic, 5)
Noise Threshol: 0.034  (12 spectra, St.Dev 0.016 + 3 * 0.0059)
Warning       : Spectral absorbances > 1000 mAU (see help for more information)
```

Figure 37: Methanol control sample, analyzed by the software automatically when the program completes or is ended by the user.

In total, each methanol sample would take approximately 10 minutes to complete running. Once the run was completed, the analysis report was again saved to a removable hard-drive and the next sample was prepared. Similar to the ethyl acetate trials, the analysis reports show that none of the collected peaks could be considered pure. An example analysis report from the first methanol sample, Methanol A (MA), from trial one is shown in figure 38 below.

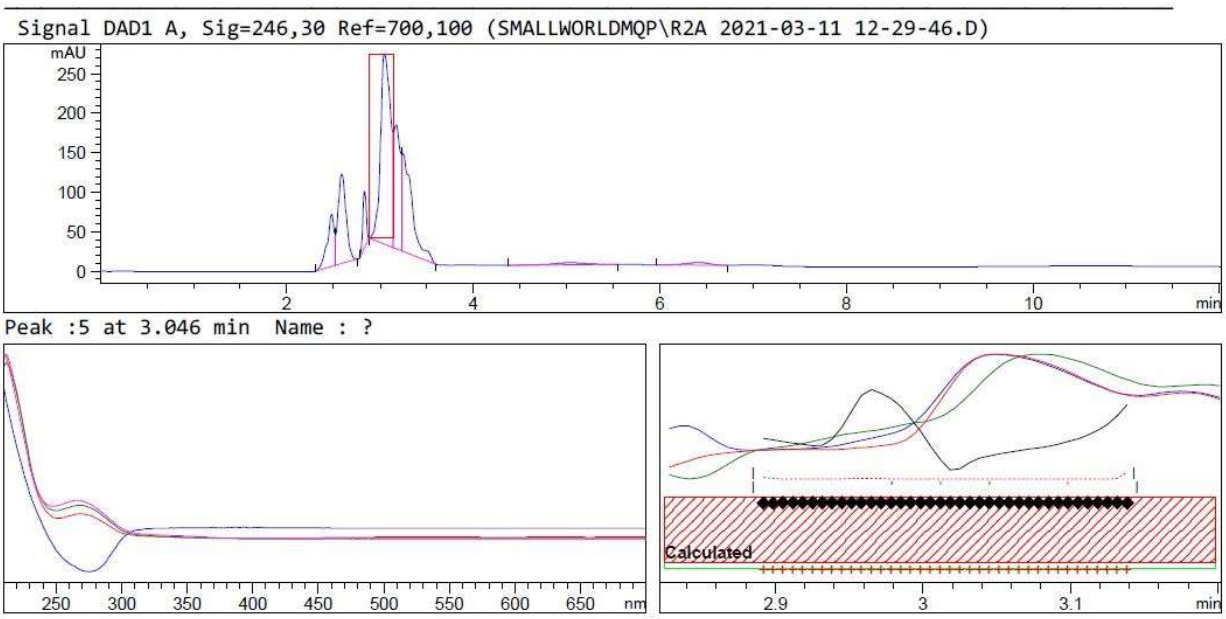


```
-> The purity factor exceeds the calculated threshold limit. <-

Purity factor : 894.320 (38 of 38 spectra exceed the calculated threshold limit.)
Threshold     : 999.983  (Calculated with 38 of 38 spectra)
Reference     : Peak start and end spectra (integrated) (2.885 / 3.145)
Spectra       : 4  (Selection automatic, 5)
Noise Threshol: 0.033  (12 spectra, St.Dev 0.0146 + 3 * 0.0062)
```

Figure 38: Analysis report for the methanol sample labelled MA. An additional warning was also reported to indicate that there were spectral absorbances present affecting the reading of spectra and subsequent calculations.

There is also supporting evidence that the methanol trials were unsuccessful in extracting our antibiotic. Despite the difference in solution, our antibiotic should elute at the same time for both the ethyl acetate and methanol samples. In both trials, the methanol samples did not have peaks around the six-to-eight-minute time frame like the ethyl acetate trials had. Additionally, as mentioned in the previous section, the organic extraction using methanol resulted in a cloudy suspension of the antibiotic in solution, which could have impacted its purity.

To better understand the results from our first two HPLC trials we also need to recognize the possible factors that have contributed to impurities in our samples. One of the main factors could be that the vials used for our trials were not new and therefore not sterile. While waiting for new vials to come in our team was instructed to clean out old vials to use. We spent time cleaning out each of the vials with pure ethanol, and then allowed them to air dry before use. This raises the question however of how efficient the ethanol cleaning was and if there were leftover impurities in the vials.

Another contributor for impurities could be leftover impurities in the column. Before running our trials, we washed the column with the same solvents used for our samples. Because we share a lab and equipment with many other students, there is a possibility that other teams used the HPLC between our samples.

Additionally, there is the possibility that what is produced by our bacteria is not a single metabolite, but multiple metabolites that work in conjunction to inhibit the growth of other bacteria. This could have been the cause for some of the impurities and appearance of multiple wavelengths of absorbance. The impurities spectra were relatively consistent eluting with what we believed to be our antibiotic. This could mean that they happen to have similar spectra or more likely that they have similar chemical structures.

There are situations when spectra are very similar or identical, but the sample is still impure. This could be due to one or more of the following situations,

- The impurity and main compound have very similar or identical spectrum
- The impurity is present in a lower concentration than the main compound
- The impurity completely coelutes with the main compound and they have identical spectrum profiles. (Stahl, 2003)

If this situation occurs, the threshold and similarity calculations can still determine the purity of the peak as they utilize all spectra within the peak. It should be noted though that the algorithms used to analyze purity of samples can only confirm the presence of impurities, it cannot prove that a peak is pure. (Stahl, 2003)

Further trials would need to be conducted to fully elaborate on our results, but these factors could explain the consistent impurities found in our HPLC trials.

4.4 Assess the Activity of the Isolated Antibiotic

The first step in assessing the activity of the purified antibiotic was to directly test our presumed antibiotic against other bacteria. After a standard incubation period of two days, the ESKAPE safe relative plates and *M. Smegmatis* plates were inspected for inhibition.

In order to keep things consistent, the antibiotic was tested against ESKAPE safe relatives and *M. Smegmatis* on both PDA and LB plates. Figures 39 and 40 below show the results from the first trial on PDA plates and LB plates, respectively.

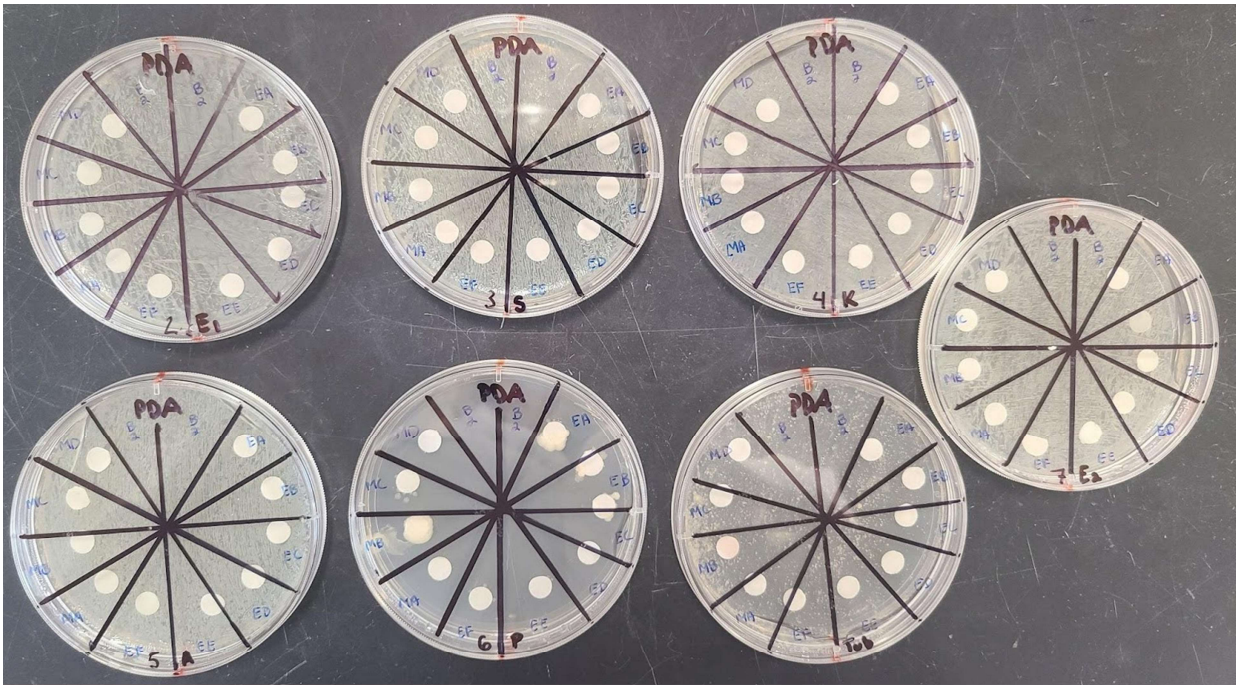

Figure 39: Results from trial one of assessing antibiotic strength against known bacteria on PDA. Each plate is labeled with the corresponding number or letter of the ESKAPE safe relative or M. Smegmatis*, and the corresponding fraction within the dedicated space.*

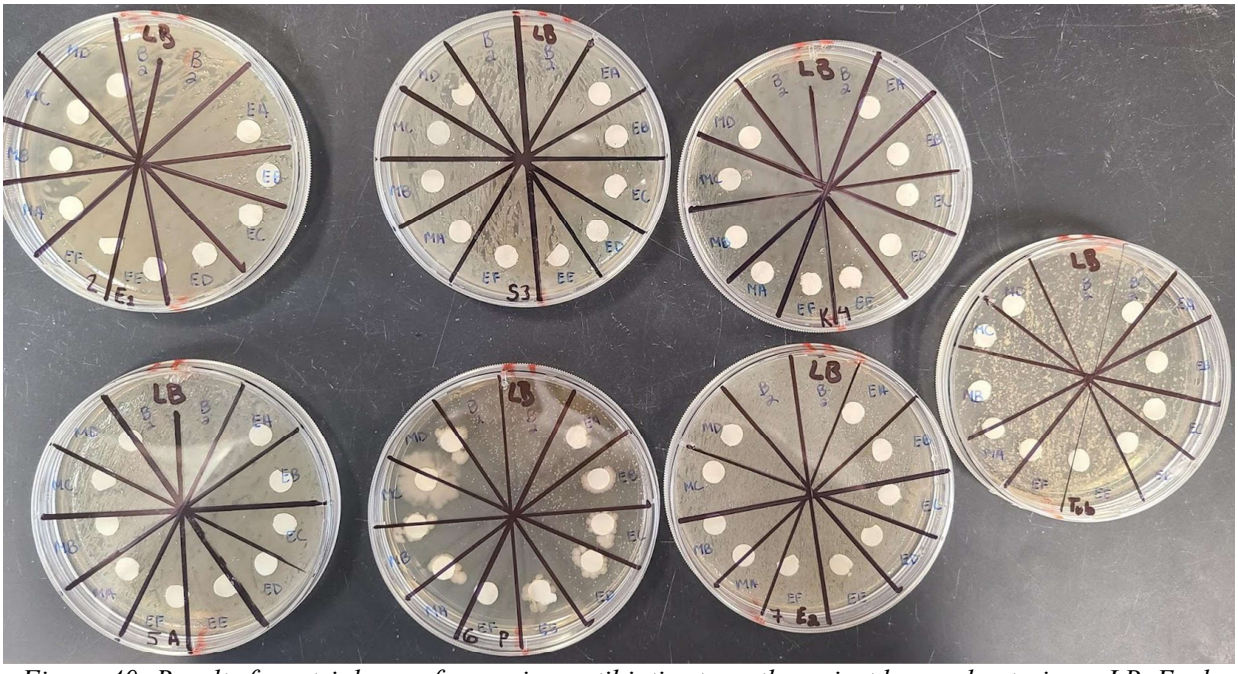

Figure 40: Results from trial one of assessing antibiotic strength against known bacteria on LB. Each plate is labeled with the corresponding number or letter of the ESKAPE safe relative or M. Smegmatis*, and the corresponding fraction within the dedicated space.*

There were no signs of inhibition from any of the fractions collected from the first trial. Knowing that 19-6 was able to inhibit some growth of different ESKAPE safe relatives and *M. smegmatis*, as seen from the spread/patch protocol in section 4.1.3, this was not an expected result. A lack of inhibition could be attributed to the poor purity of each fraction, meaning the antibiotic was not successfully isolated, as well as the unknown sterility of the disks used. The question of the disk sterility hinges on the fact that the PDA plate spread with *P. Putida* saw growth around a few of the inoculated disks; knowing *P. putida* does not grow on PDA (as seen in the positive control during the ESKAPE safe relative test of inhibition, refer to section 4.1.3), there should have been no growth on this plate at all. So, there were likely contaminants from the filter disks used that were able to grow on this media and skew our results/ability to determine the effectiveness of the antibiotic's activity. After our first trial we made our own sterile disks to ensure no contamination from outside sources.

Figures 41 and 42 below show the results from the second trial on PDA plates and LB plates respectively. Trial 2 saw potential inhibition of *A. baylyi* with the HPLC fraction labelled EA (figure 43); there appears to be a small zone of inhibition surrounding this fraction, however, no other zones of inhibition are seen for this safe relative or the other safe pathogens used for analysis. This inhibition was also not repeated in both trials, so it remains unclear as to whether this was true inhibition of the bacteria or caused by other factors.

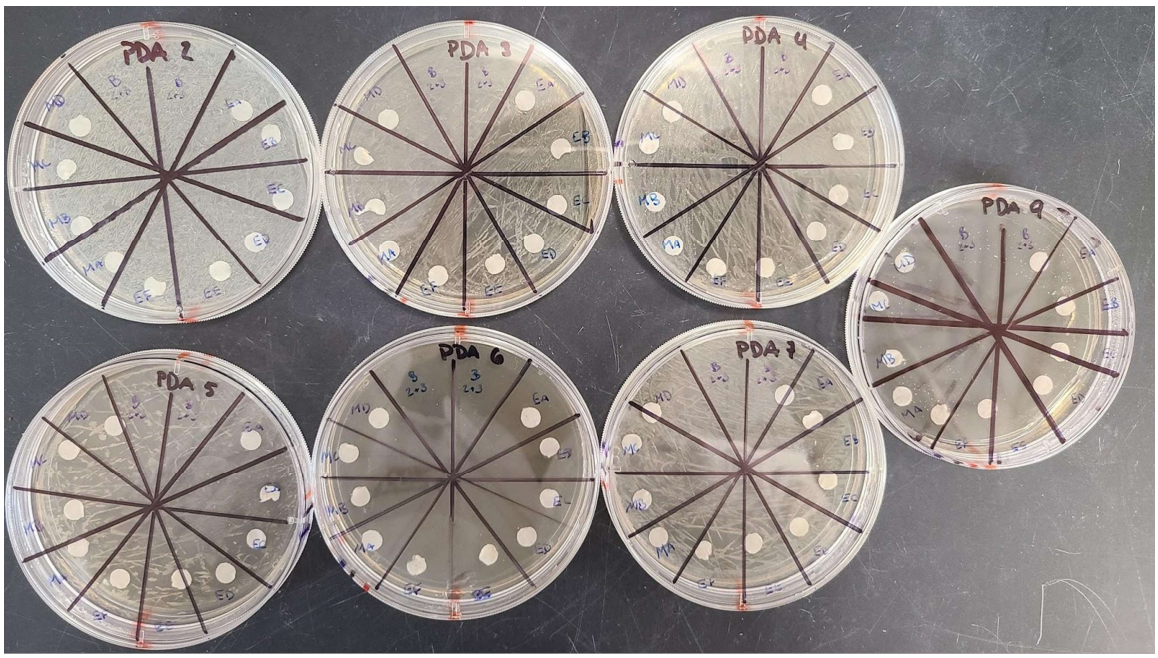

Figure 41: Results from trial two of assessing antibiotic strength against known bacteria on PDA. Each plate is labeled with the corresponding number or letter of the ESKAPE safe relative or M. Smegmatis*, and the corresponding fraction within the dedicated space.*

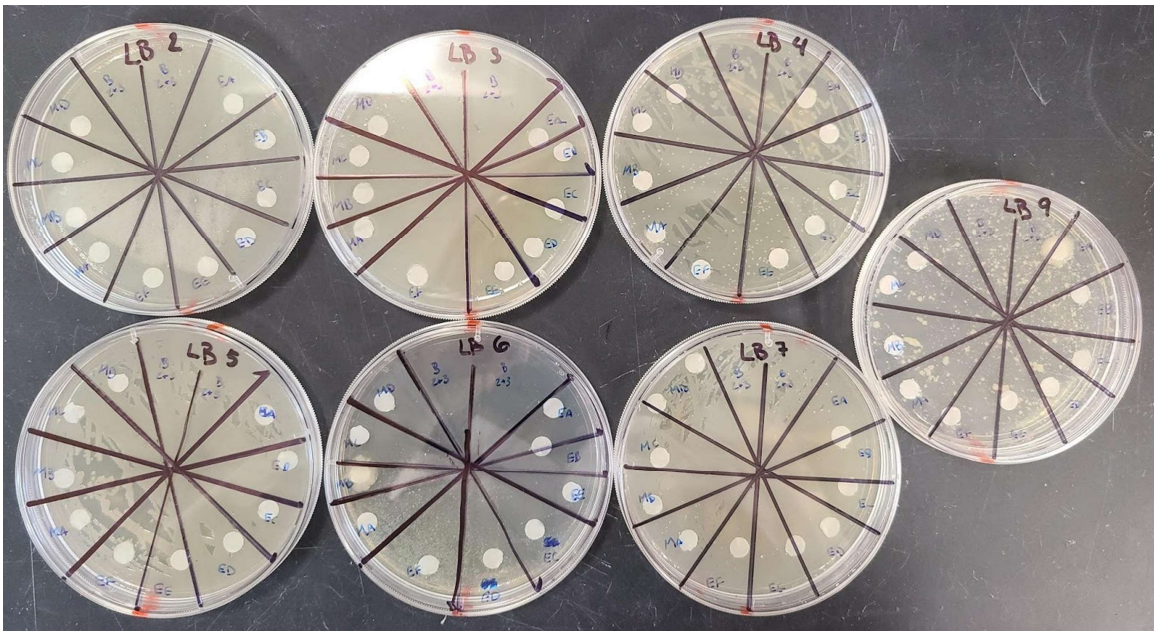

Figure 42: Results from trial two of assessing antibiotic strength against known bacteria on LB. Each plate is labeled with the corresponding number or letter of the ESKAPE safe relative or M. Smegmatis*, and the corresponding fraction within the dedicated space.*

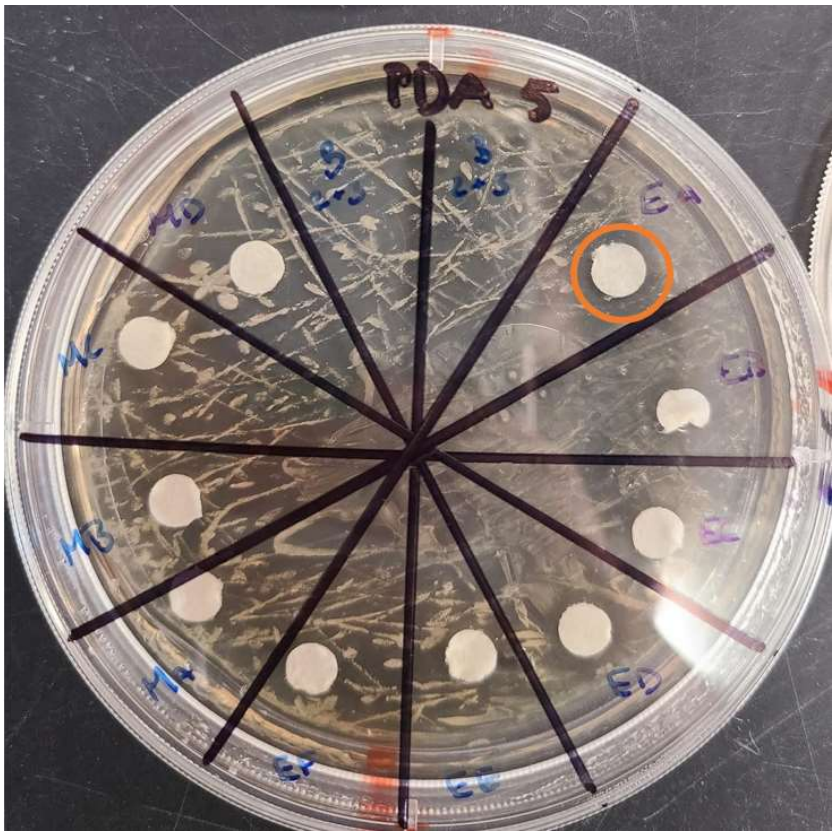

Figure 43: A close-up of the A. baylyi *PDA plate where the HPLC fraction labelled EA shows potential inhibition towards the safe relative.*

A possible reason for the ineffectiveness of the antibiotic could be that function was lost upon isolation. It is plausible that this metabolite must work in conjunction with other metabolites. And so, after purification by the organic solvents and HPLC, our antibiotic would lose its function. This would account for the lack of inhibition on most of the ESKAPE safe relative-coated and *M. smegmatis*-coated plates.

Knowing this, if time and resources had allowed, we would have liked to study an NMR spectra and performed mass spectroscopy to better understand the antibiotic's structure and function. This information could possibly answer as to why there was no inhibition after the isolate's isolation of its antibiotic; whether it be an issue with the purification process or that the isolate was never producing a viable antibiotic at all.

Section 5: Conclusion

Our MQP focuses on the production of antibiotics from soil samples. Our isolate 19-6 demonstrated a capacity to inhibit the growth of other bacteria surrounding it, and our team determined through various assays that this was likely caused by a metabolite with antibiotic properties. Yet, there were ESKAPE safe relatives that were able to grow in the presence of 19-6. This lack of inhibition proposes that the antibiotic may have specific needs, such as the employment of signaling molecules in order to be produced by 19-6. However, *M. smegmatis* was inhibited by 19-6, so there is a possibility that the antibiotic would only be effective against a select number of pathogens.

Though we were unable to identify the genus of 19-6, due to time constraints and other factors aforementioned, our team carried on experimentation without this information. We believe that for future research of 19-6, a BLAST sequencing of at least some part of 19-6's genome would give a better understanding through the comparison of known bacteria. The 16S rRNA region, if present in 19-6, may be sequenced through different primers or further adjustments to the thermocycling program. In addition to trying to amplify the 16S region, a genomic extraction sent for sequencing could provide answers to the identity of 19-6. Through the use of organic solvents and HPLC, we attempted to purify and concentrate the antibiotic from our unknown isolate. The chromatogram readings from the HPLC determined that the fractions were impure, however, we believe this could be caused by the presence of multiple metabolites. After the purified fractions failed at large to inhibit most of the ESKAPE safe relatives and *M. smegmatis,* we speculated that antibiotic activity might only occur when all metabolites work in concert. The purification process likely separated the metabolites, and ultimately caused a loss of function against ESKAPE safe relatives and *M. smegmatis*.

Overall, we believe that 19-6 is capable of producing an antibiotic to some degree. We would recommend performing NMR and mass spectroscopy in future research with this isolate to determine the structure(s), and better understand the function of the metabolites produced by 19-6.

Section 6: Appendix

Appendix A: 19-6 Origins

Our sample was taken a few feet from Salisbury Pond, Worcester, MA. This location was selected based on the assumption of its nutrient-rich environment that could habitat different microbes. The sample was collected mid-day with the soil temperature hovering around 14C. Considering how some bacteria thrive in warm, moist conditions, this area was proposed to serve as a proper breeding ground for microbial growth. Because the location chosen should be nutrient-rich, we predicted that there should be an overall high abundance in microbes. The microbes are provided with the essential nutrients to grow in this fertile soil, and these resources are ample considering the consistent input of water and sediment runoff from the pond and other surrounding factors (Hernandez, 2018).

Figure A: Site of extraction. Generally, the soil was collected from the surface level.

Figure B: The soil sample collected in the 50 mL conical tube. General observations include its darker color, and visibly grainy texture.

To select a single colony from this soil sample, we performed serial dilutions to isolate specific colonies for analysis. (Hernandez et. al, 2018, 167-171).

It was hypothesized that if the soil sample concentration is diluted, individual colonies will be easier to visualize and extract. Without dilution, the samples will grow an exponential number of colonies that grow into each other and make separating them more difficult. By reducing the concentration of the soil, we are also theoretically reducing the number of

bacteria that will grow on each plate. Fewer bacterial colonies will make it easier to discern which colonies are which, and ensure that upon extraction, we are picking a single colony for analysis.

After a standard growth period, the more concentrated plates experienced the most microbial growth, and the less concentrated plates showed little growth with ample room between colonies on the plate. Both types of media, LB and PDA, experienced some colonies with zones of inhibition. Individual colonies may be identified in this way (by looking for zones of inhibition, bacteria growing in a curved pattern around a single colony) or by identifying colonies that seem to be growing away/separate from other colonies that are growing/mixing into each other.

Figure C: Diluted (10^-1) LB plate. Experienced the most microbial growth, the red dots are colonies that exhibit possible zones of inhibition. These zones either displayed colonies growing in a curve-like fashion around a specific colony, or a colony that is surrounded by other colonies but does not come into direct contact with the surrounding colonies.

Figure D: Diluted (10^-5) LB plate. Experienced limited microbial growth due to less concentrated soil, however one of the colonies did experience a possible zone of inhibition where the surrounding bacteria curve around the 'red' colony (colony of speculation is spotted with a red dot).

Next, to further select colonies with potential antibiotic-producing capabilities using the pick and patch protocol, where we selected potential candidates for antibiotic production and transferred them to a ‘master’ plate where they were grown together separately from the rest.

Each type of media experienced some sort of zone of inhibition. However, only about 7 of the isolates formed what could be considered a zone of inhibition, with its surrounding isolates either growing in curved fashion around the isolate in question or leaving some sort of space between its neighboring isolates.

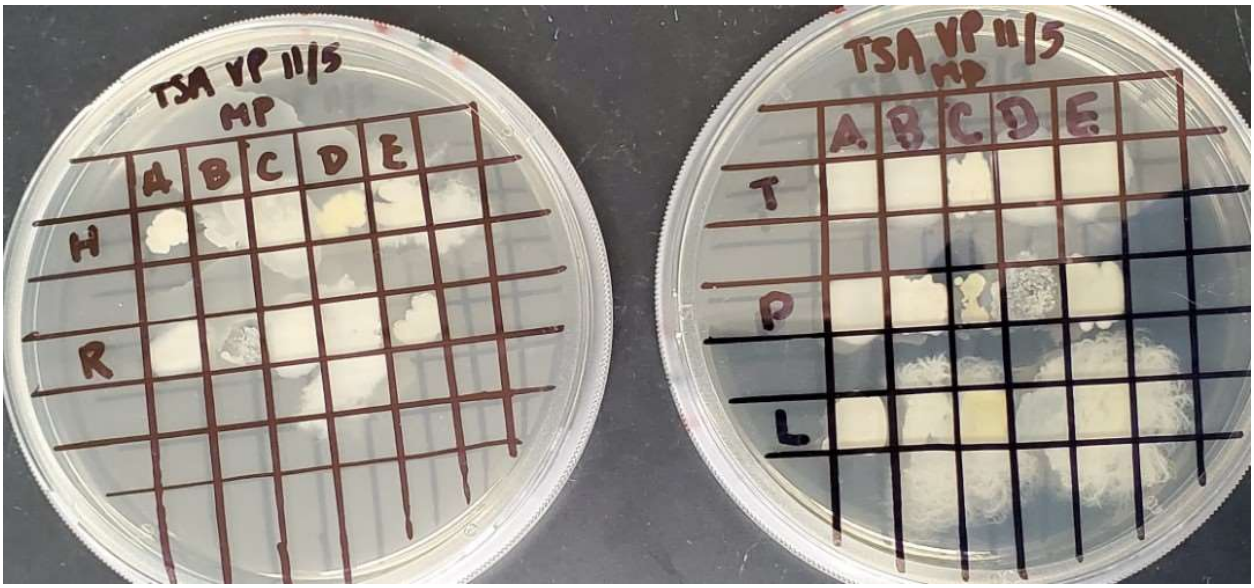

Figure E: Only a select few of these isolates produced a zone of inhibition. The others simply grew into each other and did not inhibit the growth of its neighboring isolates.

Appendix B: 19-6 Initial ESKAPE Safe Relative Inhibition

To test the potential antibiotic-producing qualities of the isolates that showed possible zones of inhibition on the master plate, our group grew these isolates together with known ESKAPE safe relatives. If the selected isolates were able to inhibit the growth of these safe relatives, it is likely that they may be producing an antibiotic. To test this potential, the following protocol was carried out:

Obtained the master plate and a liquid culture with an ESKAPE safe relative provided in the lab (*Pseudomonas putida*).

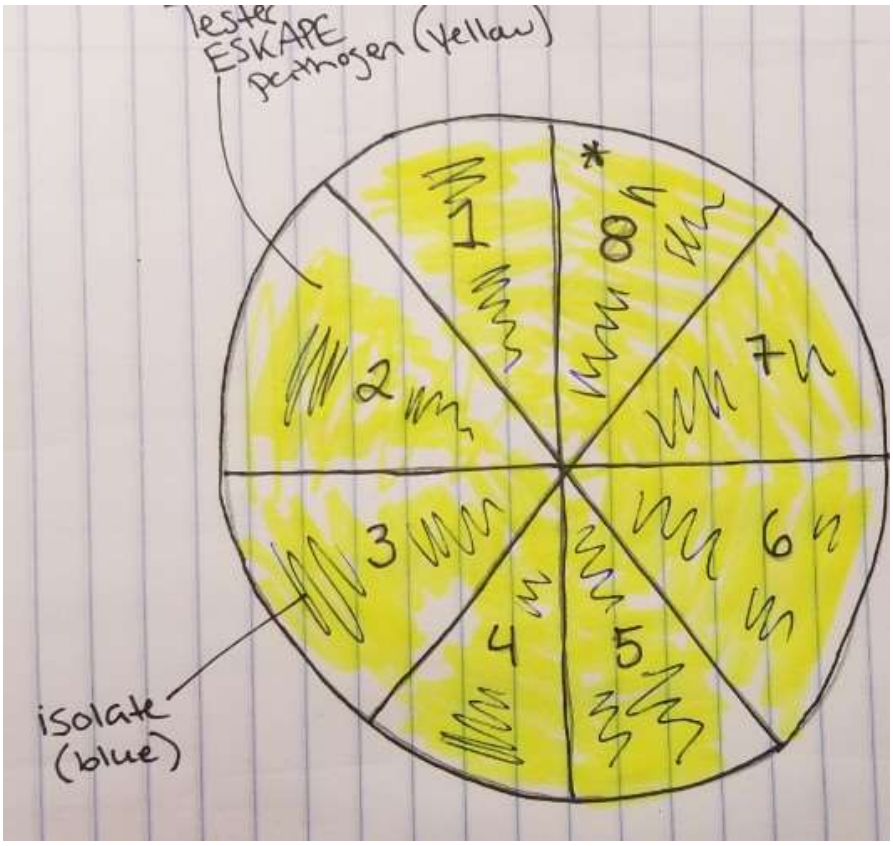

Figure F: A schematic of the spread/patch plates used in this experiment with the ESKAPE tester strain (yellow) is spread uniform all over the plate, and each isolate (blue) is spread across the tester strain in designated areas.

The isolates labelled 4 and 7 showed a zone of inhibition against the *P. putida* that relates to a potential antibiotic-producing bacterium that is able to prevent the growth of this safe relative. These isolates were able to be further characterized; isolate 7 was arbitrarily selected for different chemical assays.

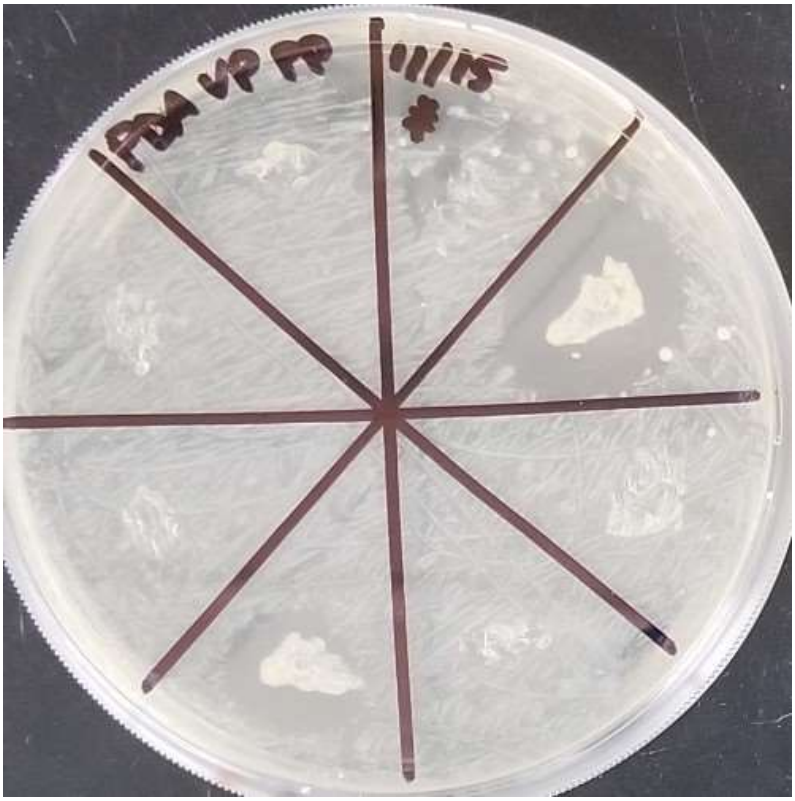

Figure G: The PDA plate showed resistance to the safe relative, P. putida, with the isolates 4 and 7 (PE and RE, respectively).

Appendix C: Chemical Assays 19-6

All references were taken/based off of the procedures described in Hernandez, S., Tsang, T., Bascom-Slack, C., Broderick, N., and Handelsman, J. (2018). Tiny earth: A research guide to studentsourcing antibiotic discovery. Michigan: XanEdu. Print.

Gram-staining is used to distinguish if the bacterium in question is gram-negative/positive. Gram-stains tell us about the composition of the bacteria's membrane and provides insight into the bacteria's antibiotic-producing capabilities. Used a simple staining method to characterize the isolate (Buckholt, 2019).

The isolates stain had a purplish coloration and was therefore deemed gram-negative. Gram-negative bacteria are typically associated with antibiotic-producing capabilities. This gram-stain can be confirmed with a MacConkey plate test.

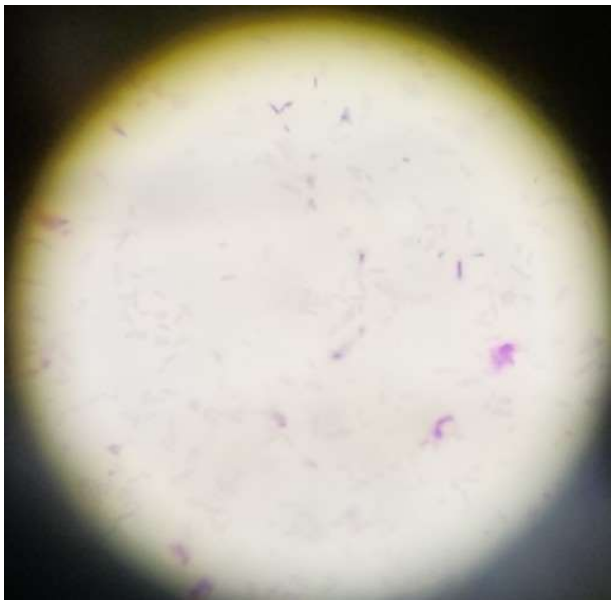

Figure H: The above images depict the isolate 7 under oil immersion after treatment of gram staining procedures. The stain is purplish indicating a gram-negative bacterium.

The following chemical assays include protocols, interpretations of results, and the experimental results that further characterized the isolate 7.

MacConkey Experimental design:

Streak a MacConkey's agar plate with pure isolated culture. Ensure colonies are well separated to better identify lactose fermentation through observations of color change (Buckholt, 2019).

The media surrounding the gram-negative bacteria will change color depending on its fermentation of lactose. If the isolate is strongly lactose-fermenting, the colony will appear pinkish/red and have a pink ring around it, whereas weakly lactose-fermenting isolates will appear pinkish/red but will not have a pink ring. Colonies that do not ferment lactose will be colorless on the agar, and the surrounding media will be transparent. This colorization is caused by the lactose-fermenting colonies secreting a bile acid that lowers the pH of the medium which is detected by a pink/red coloration around the colonies on the agar (Buckholt, 2019).

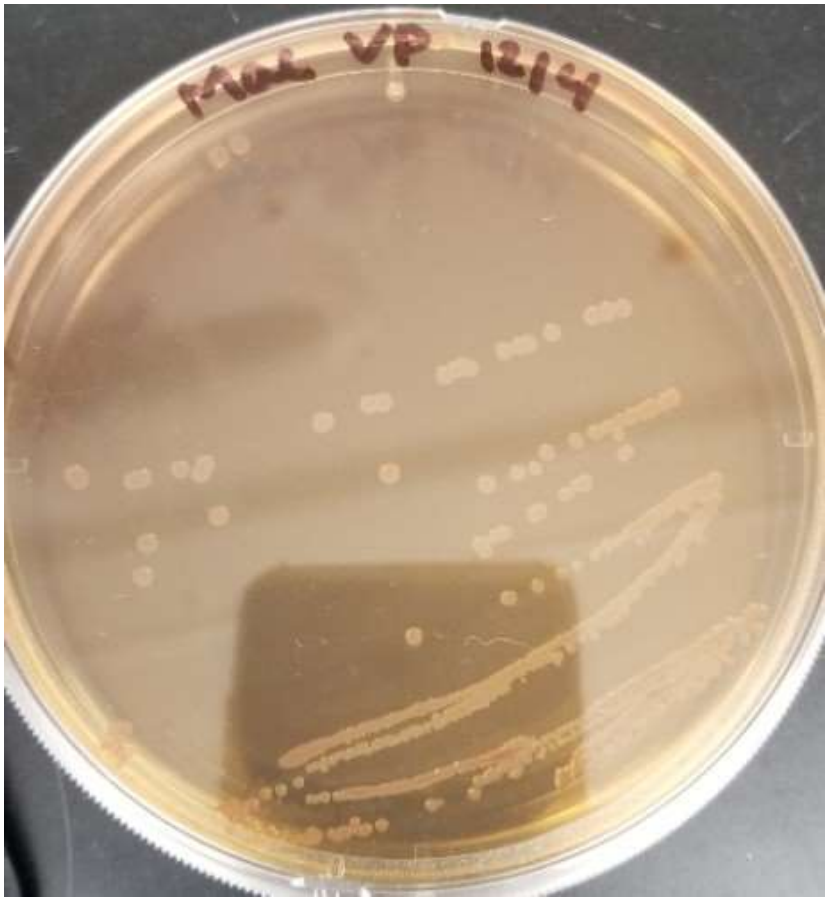

Figure I: MacConkey plate after incubation period. No color change appeared indicating no lactose fermentation (lactose negative). The isolate did, however, grow therefore the isolate is confirmed as gram-negative.

Triple Sugar Iron Experimental design:

Streak triple sugar iron agar with pure culture and observe for distinct colorization to determine if the isolate is fermenting the different sugars. Stab TSI tubes with pure isolates. Incubate tubes at 35 degrees C for 24 hours. Observe color change and identify sugar fermentation through observations of color change (Buckholt, 2019). During fermentation, the bacteria will excrete acid which lowers the pH of the surrounding media. Lower pH yields a color change of red/orange to yellow; higher pH yields a color change into a deep red. H_2S-positive bacterium will reduce the sulfite in the agar to sulfide which then reacts with iron and causes black FeS to precipitate out (Buckholt, 2019).

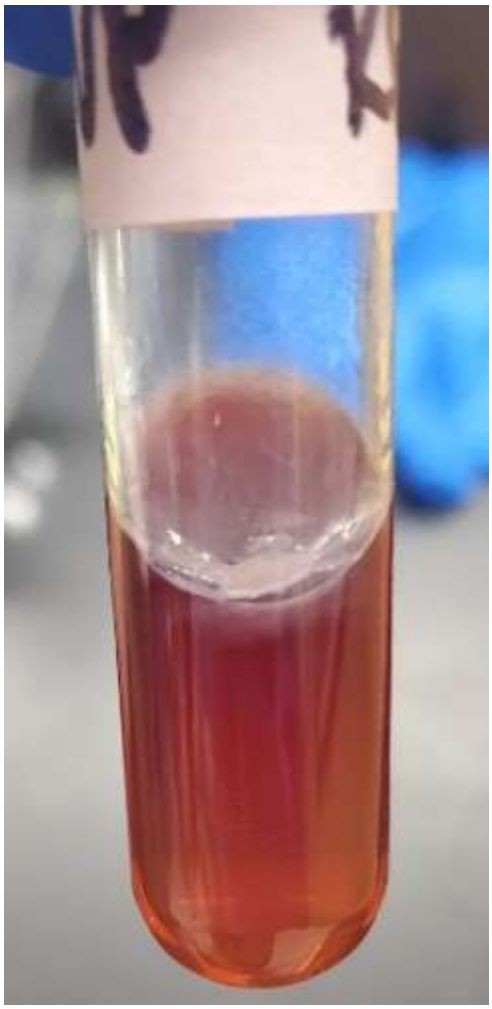

Figure J: TSI tube after incubation period. The coloration appeared red/red indicating that there was no fermentation of any kind taking place, and there was no formation of a black precipitate so H_2S was not being produced/reacted with.

Motility and Indole Experimental design:

Observe for chemical reactions after incubating inoculated MIL tubes with pure isolates. Stab MIL tubes with pure isolates. Incubate tubes at 35 degrees C for 24 hours. Examine tubes for evidence of lysine deaminase, motility, lysine decarboxylase reactions. Add indole reagent kovacs, and observe for indole production (Buckholt, 2019). The production of lysine deaminase is detected by a red/brown colorization. Motility displays clouding of the agar or growth starting from the point of inoculation. Lysine decarboxylase production creates a purple color throughout the agar. Lysine-negative colonies make the medium yellow that could be red/purple on the top portion.

After adding 4 drops of indole reagent kovacs to each tube, a pinkish/red color indicates a positive indole test (Buckholt, 2019).

E. coli has tested positive for lysine decarboxylase, motility and indole production making it a positive control for these reactions; it has also tested negative for lysine deaminase making it a negative control for this chemical reaction. *P. alcalifaciens* tested positive for

motility and lysine deaminase and therefore is a positive control for these reactions and is a negative control for lysine decarboxylase and indole production. Meanwhile, *S. flexneri* is an overall negative control because it tests negative for all four reactions. (Refer to table below for production schematic).

Table A: ESKAPE Table

ORGANISM	ATCC™	LYSINE DECARBOXYLASE	MOTILITY	LYSINE DEAMINASE	INDOLE PRODUCTION
Escherichia coli	25922	+	+	–	+
Providencia alcalifaciens	9886	–	+	+	–
Salmonella enterica subsp. enterica serotype Enteritidis	13076	+	+	–	–
Shigella flexneri	12022	–	–	–	–

Table of biochemical reaction productions for known bacteria (Buckholt, 2019).

Figure K: MIL tube after incubation period. A deep purple ran throughout the tube initially. After adding the indole reagent, the tube had white at the top with purple down the rest of the tube (shown above). Coloration shows lysine positive and indole negative, respectfully.

Catalase Experimental design:

Treating the isolate with hydrogen peroxide (H_2O_2) to test for catalase production through the observation of bubble formation. Using a sterile inoculating loop, pick a single colony from the master plate of isolate. Steak isolate in a zig-zag fashion onto the center of the slide until the smear becomes visible. Smear three isolates per slide as separate as possible. Using a pipette, place 1 drop of 3% H_2O_2 onto smear. Observe for air bubble formation (Buckholt, 2019). Rapid bubble formation indicates a positive reaction that is the isolate is producing catalase which is decomposing H_2O_2 into water and oxygen; a weak reaction of little/slow bubble formation or no bubbles indicates a negative reaction where catalase production is low or non-existent (Buckholt, 2019).

Figure L: Catalase reactions, the control (E. coli) is catalase positive and therefore reacts to break down hydrogen peroxide and form bubbles (shown at left). The isolate (at right) shows no bubble formation and therefore is not reacting to the hydrogen peroxide to form catalase.

Amylase/Starch Experimental design

Culturing isolate on a starch agar plate to test for reactions with iodine. Inoculated starch agar plate with isolate using sterile loop in single line down the center of the plate. Fatter lines show the best/most clear results. Do not streak for isolated colonies. Culture plate for two days, and flood plate with Gram's iodine and observe for color change. Observations should be made with haste as the colors fade quickly (Buckholt, 2019).

Inoculated starch plates that are flooded will show a reaction between the iodine and starch through the formation of a blue complex. The starch around the colony will become clear if it is degraded (and depletes the area of starch so that iodine can no longer react with anything in that area around the colony. Amylase is degrading the starch in this case and produces the image shown below. This starch assay works in the inverse of the amylase assay. That is if the isolate tests positive for amylase and appears as the image below, then it also tests negative for starch (and vice versa). If no clear area is shown around the colony, then the colony is amylase negative and does not degrade the starch in the presence of iodine (Buckholt, 2019).

Figure M: A positive amylase test shown by the clear portion near the isolate being tested (Buckholt, 2019).

Figure N: Starch plate flooded with iodine. No clear colorization visible around line of growth, therefore amylase negative and starch positive.

Oxidase Experimental design

Added oxidase reagent to isolate samples to observe for color change indicating oxidizing potential of aromatic amines of colonies. Transferred isolate to a microscope slide. Obtain reagent from the microfuge tubes inside a small box located in the front of the classroom or provided by your lab instructor. Add a drop of reagent to isolate and observe color change (Buckholt, 2019).

After adding oxidase reagent to the colony, if the colony turns into a deep purple color, the colony is oxidase positive. This means that the colony is able to oxidize aromatic amine compounds. However, no color change, that is the colony stays the blue color of the oxidase reagent (the color the reagent turns when exposed to light) then the isolate is oxidase negative and does not have oxidizing capabilities of aromatic amine groups (Buckholt, 2019).

Figure O: A before (left) and after (right) image of an oxidase positive isolate before/after a drop of oxidase reagent was added. Notice the deep purple indicating the oxidizing potential of the isolate (Buckholt, 2019).

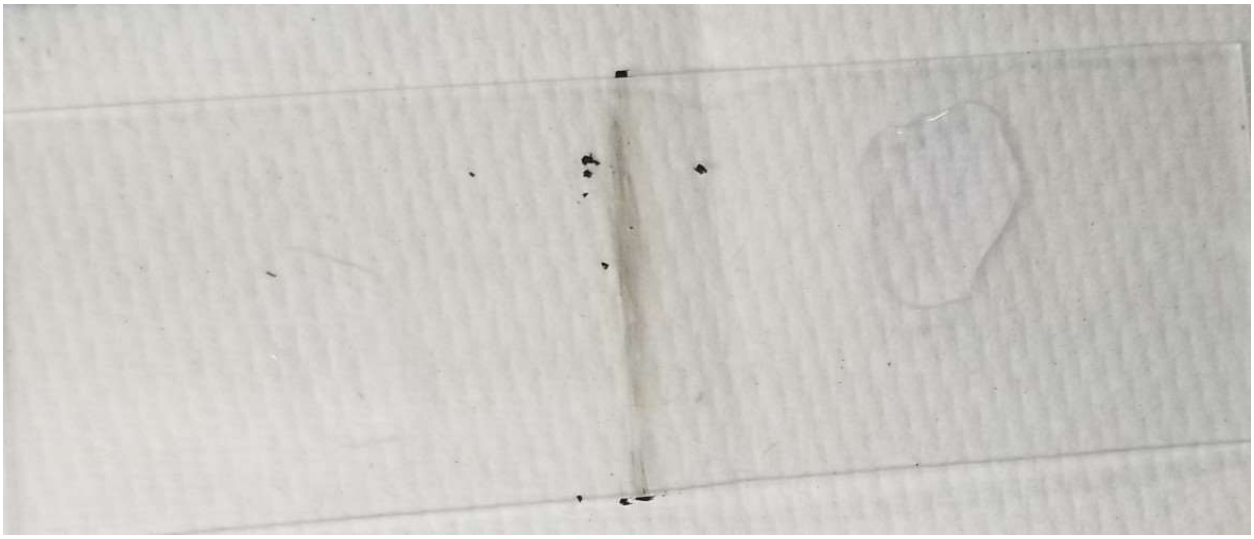

Figure P: Oxidase reactions, the control (E. coli) did not show a color change because it does not oxidize amines (at left); isolate 7 is also oxidase negative and did not show the color change indicative of the oxidation of aromatic amine compounds from the oxidase reagent (at right).

Overall Discussion of Chemical Assays:

The isolate being both oxidase and catalase negative tells us two unique factors considering its catalytic properties. That is that our isolate is not able to oxidize aromatic amine compounds. Oxidation gives way to a variety of chemical reactions; our isolates low oxidation rates of amines could potentially offer us information on other chemical reactions/pathways that the isolate performs. The isolate is also unable to produce catalase, this makes the isolate prone to the destructive nature of peroxides (hydrogen peroxide).

Without this defense mechanism, our isolate may rely on other reactions to prevent its denaturation from harmful compounds.

The isolate 7 has been categorized as gram negative via the gram staining technique shown in figure H. This relates to the composition of the cell wall for our isolate, corresponding to a thin peptidoglycan cell wall. The MacConkey plate has confirmed that the isolate is indeed gram negative as suggested by the gram stain. This isolate's morphology characterized it as circular in shape with a raised elevation, and an entire margin. Most of the biochemical assays turned out negative, indicating a low fermentation quality of the enlisted compounds. The isolate does not ferment many compounds and must produce compounds such as organic products and ATP in other ways (perhaps aerobically). These assays can be used to support the identification of the isolate once it is cross referenced to a known bacterium.

Section 7: References

Addgene. (2018, February 20). *Agarose gel electrophoresis.* Addgene. https://www.addgene.org/protocols/gel-electrophoresis/

Adrizain, R., Suryaningrat, F., Alam, A., & Setiabudi, D. (2018, March). Incidence of multidrug-resistant, extensively drug-resistant and pan-drug-resistant bacteria in children hospitalized at Dr. Hasan Sadikin general hospital Bandung Indonesia. https://iopscience.iop.org/article/10.1088/1755-1315/125/1/012077/meta

Alós, J.-I. (2015). [Antibiotic resistance: A global crisis]. Enfermedades Infecciosas Y Microbiología Clínica, 33(10), 692–699. https://doi.org/10.1016/j.eimc.2014.10.004

Bacteria cell structure. (2015, November 13). Molecular Expressions: Cell biology and microscopy structure and function of cells and viruses. https://micro.magnet.fsu.edu/cells/bacteriacell.html

Royer, C., & Ball, R. (2019). *Ronan Ball and Cole Royer MQP 2019 - BBT Department.* : Worcester Polytechnic Institute.

Bengtsson-Palme, J., Kristiansson, E., & Larsson, D. G. J. (2018). Environmental factors influencing the development and spread of antibiotic resistance. FEMS Microbiology Reviews, 42(1). https://doi.org/10.1093/femsre/fux053

Bertrand, R.L. (2019). Lag phase is a dynamic, organized, adaptive, and evolvable period that prepares bacteria for cell division. *Journal of Bacteriology, 7(201)*, 1-21. https://doi.org/10.1128/JB.00697-18.

Bruslind, L. (2021, January 3). *Bacteria - Cell Walls*. Oregon State University. https://bio.libretexts.org/@go/page/10632

Buckholt, M. (2019). *Catalase test*. Labarchives. https://mynotebook.labarchives.com/.

Buckholt, M. (2019). *Gram and simple stain procedures*. Labarchives. https://mynotebook.labarchives.com/.

Buckholt, M. (2019). *MacConkey agar test.* Labarchives. https://mynotebook.labarchives.com/.

Buckholt, M. (2019). *Motility and indole test*.Labarchives. https://mynotebook.labarchives.com/.

Buckholt, M. (2019). *Oxidase test*.Labarchives. https://mynotebook.labarchives.com/

Buckholt, M. (2019). *Starch assay/Amylase test*.Labarchives. https://mynotebook.labarchives.com/

Buckholt, M. (2019). *Triple sugar iron agar (TSI agar)*.Labarchives. https://mynotebook.labarchives.com/

Bush, K., Courvalin, P., Dantas, G., Davies, J., Eisenstein, B., Huovinen, P., Jacoby, G. A., Kishony, R., Kreiswirth, B. N., Kutter, E., Lerner, S. A., Levy, S., Lewis, K., Lomovskaya, O., Miller, J. H., Mobashery, S., Piddock, L. J. V., Projan, S., Thomas, C. M., & Zgurskaya, H. I. (2011). Tackling antibiotic resistance. *Nature Reviews Microbiology*, 9(12), 894–896. https://doi.org/10.1038/nrmicro2693

CDC. (2020, March 13). What Exactly is Antibiotic Resistance? Centers for Disease Control and Prevention. https://www.cdc.gov/drugresistance/about.html

Chaudhary, A. S. (2016). A review of global initiatives to fight antibiotic resistance and recent antibiotics′ discovery. *Acta Pharmaceutica Sinica B, 6(6),* 552–556. https://doi.org/10.1016/j.apsb.2016.06.004

Clardy, J, & Walsh, C. (2004). Lessons from natural molecules. *Nature Publishing Group. 432,* 829-837. doi:10.1038/nature03194

Davies, J., & Davies, D. (2010). Origins and evolution of antibiotic resistance. *Microbiology and Molecular Biology Reviews: MMBR, 74(3)*, 417–433. https://doi.org/10.1128/MMBR.00016-10

Delcour, A.H. (2009). Outer membrane permeability and antibiotic resistance. *Biochimica et Biophysica Acta,* 808-816. Doi: 10.1016/j.bbapap.2008.11.005

Fernandes, P., & Martens, E. (2017). Antibiotics in late clinical development. *Biochemical Pharmacology*, *133,* 152–163. https://doi.org/10.1016/j.bcp.2016.09.025

Fischbach, M. A., & Walsh, C. T. (2009). Antibiotics for Emerging Pathogens. *Science, 325(5944)*, 1089-1093. doi:10.1126/science.1176667.
Fischbach, M.A., Walsh, C.T., & Clardy J. (2008). The evolution of gene collectives: How natural selection drives chemical innovation. *PNAS. 105(12),* 4601-4608. doi10.1073pnas.0709132105
Frank, J.A., Reich, C.I., Sharma, S., Weisbaum, J.S., Wilson, B.A., & Olsen, G.J. (2008). Critical evaluation of two primers commonly used for amplification of bacterial 16S rRNA genes. *Applied and Environmental Microbiology, 74(8),* 2461-2470. Doi: 10.1128/AEM.02272-07
Frieri, M., Kumar, K., & Boutin, A. (2017). Antibiotic resistance. *Journal of Infection and Public Health, 10(4)*, 369–378. https://doi.org/10.1016/j.jiph.2016.08.007
Gould, K. (2016). Antibiotics: From prehistory to the present day. J*ournal of Antimicrobial Chemotherapy, 71(3)*, 572–575. https://doi.org/10.1093/jac/dkv484
Grant, S. S., & Hung, D. T. (2013). Persistent bacterial infections, antibiotic tolerance, and the oxidative stress response. *Virulence, 4(4)*, 273–283. https://doi.org/10.4161/viru.23987
Hernandez, S., Tsang, T., Bascom-Slack, C., Broderick, N., & Handelsman, J. (2018). *Tiny Earth- A research guide to studentsourcing antibiotic discovery.* Michigan: XanEdu. Print.
Hutchings, M. I., Truman, A. W., & Wilkinson, B. (2019). Antibiotics: Past, present and future. *Current Opinion in Microbiology, 51,* 72–80. https://doi.org/10.1016/j.mib.2019.10.008
Integrated DNA Technologies. (2021). *ReadyMade™ Primers.* IDT: Integrated DNA Technologies. https://www.idtdna.com/pages/products/custom-dna-rna/readymade-inventoried-oligos/readymade-primers
Janda, J.M. & Abbott, S.L. (2007). 16S rRNA gene sequencing for bacterial identification in the diagnostic laboratory: Pluses, perils, and pitfalls. *Journal of Clinical Microbiology, 45(9)*, 2761-2764. doi:10.1128/JCM.01228-07
Laxminarayan, R., Duse, A., Wattal, C., Zaidi, A. K. M., Wertheim, H. F. L., Sumpradit, N., Vlieghe, E., Hara, G. L., Gould, I. M., Goossens, H., Greko, C., So, A. D., Bigdeli, M., Tomson, G., Woodhouse, W., Ombaka, E., Peralta, A. Q., Qamar, F. N., Mir, F., &Cars, O. (2013). Antibiotic resistance—The need for global solutions. *The Lancet Infectious Diseases, 13(12),* 1057–1098. https://doi.org/10.1016/S1473-3099(13)70318-9
Mendelsohn, J. A. (2002). "Like All That Lives": Biology, Medicine and Bacteria in the Age of Pasteur and Koch. *History and Philosophy of the Life Sciences, 24(1)*, 3–36. Doi: 10.1080/03919710210001714293
Oldfield, E., & Feng, X. (2014). Resistance-resistant antibiotics. *Trends in Pharmacological Sciences, 35(12)*, 664–674. https://doi.org/10.1016/j.tips.2014.10.007
Raetz C.R.H., & Whitfield, C. (2002). Lipopolysaccharide Endotoxins. *Annual Review Biochemistry, 71,* 637-700. 10.1146/annurev.biochem.71.110601.135414
Romaniuk, J.A.H., & Cegelski, L. (2015). Bacterial cell wall composition and the influence of antibiotics by cell-wall and whole-cell NMR. *Philosophical Transactions of the Royal Society B, 370,* 1-14. http://dx.doi.org/10.1098/rstb.2015.0024
Romero, D., Traxler, M. F., López, D., & Kolter, R. (2011). Antibiotics as Signal Molecules. *Chemical Reviews, 111(9),* 5492–5505. https://doi.org/10.1021/cr2000509
Sabtu, N., Enoch, D. A., & Brown, N. M. (2015). Antibiotic resistance: what, why, where, when and how?. *British Medical Bulletin*, *116*, 105–113. https://doi.org/10.1093/bmb/ldv041
Stahl, M. (2003). Peak purity analysis in HPLC and CE using diode-array technology. *Agilent technologies.* https://www.agilent.com/
Stoll, D.R., Rutan, S.C., & Venkatramani, C.J. (2018). Peak purity in liquid chromatography part I: Basic concepts, commercial software, and limitations. *LCGC North America, 36(2),* 100-110. https://www.chromatographyonline.com/view/peak-purity-liquid-chromatography-part-i-basic-concepts-commercial-software-and-limitations
Strobel, G., & Daisy, B. (2003). Bioprospectin for microbial endophytes and their natural products. *American Society for Microbiology, 67(4),* 491-502. https://dx.doi.org/10.1128%2FMMBR.67.4.491-502.2003

Tacconelli, E., Carrara, E., Savoldi, A., Harbarth, S., Mendelson, M., Monnet, D. L., Pulcini, C., Kahlmeter, G., Kluytmans, J., Carmeli, Y., Ouellette, M., Outterson, K., Patel, J., Cavaleri, M., Cox, E. M., Houchens, C. R., Grayson, M. L., Hansen, P., Singh, N., & Zorzet, A. (2018). Discovery, research, and development of new antibiotics: The WHO priority list of antibiotic-resistant bacteria and tuberculosis. *The Lancet Infectious Diseases, 18(3)*, 318–327. https://doi.org/10.1016/S1473-3099(17)30753-3

Voet, D., Voet, J. G., & Pratt, C. W. (2016). Fundamentals of Biochemistry: Life at the Molecular Level (5th edition). Hoboken, NJ: John Wiley & Sons.

Wizard Genomic DNA Purification Kit. (2019). Promega Corporation. Print.

Wobbe, R. (2015). Methods for Purifying and Analyzing Antibacterial Compounds using High-Pressured Liquid Chromatography. Worcester Polytechnic Institute- Department of Chemistry and Biochemistry.

World Health Organization (Ed.). (2014). Antimicrobial resistance: Global report on surveillance. World Health Organization. https://apps.who.int/iris/bitstream/handle/10665/112642/9789241564748_eng.pdf;jsessionid=A2BF8D8A9939ADB861F65CD8C282B31C?sequence=1

Yaghoubi, A., Khazaei, M., Jalili, S., Hasanian, S. M., Avan, A., Soleimanpour, S., & Cho, W. C. (2020). *Bacteria as a double-action sword in cancer. Biochimica et Biophysica Acta (BBA) - Reviews on Cancer, 1874(1)*. https://doi.org/10.1016/j.bbcan.2020.188388